Highlights

- 1,8-naphthalimides can be materialized by introducing electron-donating or electron-accepting units at the C-4 position.
- Many 4-substituted 1,8-naphthalimide derivatives were capable to form glasses (up to 254 ^{o}C).
- Some of them displayed relatively good charge-transporting capabilities
- 1,8-naphthalimides are used in OLEDs, organic solar cells etc.

A review of investigation on 4-substituted 1,8-naphthalimide derivatives

Dalius Gudeika[a,b*], Juozas V. Grazulevicius[a]

[a] *Department of Polymer Chemistry and Technology, Kaunas University of Technology, Radvilenu pl. 19, LT-50254, Kaunas, Lithuania*

[b] *Institute of Solid State Physics, University of Latvia, 8 Kengaraga St., Riga LV-1063, Latvia*

*Corresponding author. E-mail: gudeika.dalius@gmail.com (Dalius Gudeika)

Abstract

In the recent years, much attention has been paid to the design and synthesis of new 4-substituted 1,8-naphthalimide architectures as well as to the studies of the properties of the materials. Wide possibilities of changing the optical and fluorescence, thermal, electrochemical, electroluminescent, and photoelectrical properties of 1,8-naphthalimide derivatives can be materialized by introducing different electron-donating or electron-accepting substituents at the C-4 position in the 1,8-naphthalimide moiety. Many 4-substituted 1,8-naphthalimide derivatives were capable to form glasses (up to 254 ^{o}C) with good morphological stability. Moreover, some of them displayed relatively good charge-transporting capabilities that were appropriated for balanced carrier injection in organic light-emitting diodes. At the same time, derivatives 1,8-naphthalimide have found application in other optoelectronic devices, such as organic solar cells, as well as in memory devices. This review article appeals to researchers, students and professionals who are interested in the synthesis studies and applications of 4-substituted 1,8-naphthalimides.

Keywords: 1,8-naphthalimide, C-4 position, electron-donating, electron-accepting, optoelectronic devices.

1. Introduction

So far, the use of the concept of electron-accepting and donating (A-D) system in 1,8-naphthalimide chemistry was rather limited. In the recent years the interest in the optical and fluorescence, eletrochemical and photoelectrical properties of 1,8-naphthalimide derivatives has been steadily increasing [1,2,3]. Introduction of an electron-donating moiety at the C-4 position of 1,8-naphthalimide compounds generate intramolecular charge transfer (ICT) excited state [4,5] and leads to a large bathochromic shift in both absorption and emission spectra.

Furthermore, naphthalimide derivatives have high electron affinity due to the existence of an electron-deficient centre [6,7,8], however the oxidation and reduction potentials of 1,8-naphthalimides can be tuned by substitution. These derivatives display good electron-transporting or hole-blocking capabilities that are appropriate for balanced carrier injection in organic light-emitting diodes (OLEDs). Searching for new effective charge transporting materials for optoelectronic devices it is of interest to synthesize and study 1,8-naphthalimide derivatives with desirable hole, electron or ambipolar charge transporting properties.

There is a substantial number of studies on perylene diimide derivatives and on their optoelectronic applications. Over the last decades, academic and industrial interest in this class of chromophores has increased. However no other reviews was done on 1,8-naphthalimide derivatives since these compounds possess unique optical, electrochemical, and electronic properties. The present review focuses on the progress and development of 4-substituted 1,8-naphthalimide derivatives for applications in optoelectronics with respect to the change in molecular structures, energy levels etc. The investigation

of the 4-substituted 1,8-naphthalimide derivatives demonstrate that many of these materials have charge transporting abilities and show film forming properties. These properties make naphthalimides the potential materials for the applications in optoelectronics, such as coloration of polymers [9], laser active media [10], photosensitive biological units [11], fluorescent markers in biology [12], OLEDs [13,14], photoinduced electron transfer sensors [15], fluorescence switchers [16], liquid crystal displays [17], strongly absorbing and colorful dyes [18], ion probes [19].

2. 1,8-Naphthalimide derivatives with aromatic substituents at the 4-position

Many studies were reported on 1,8-naphthalimide derivatives, however it is still meaningful to extend the research the derivatives, introducing new electron-donating and electron-accepting groups at the C-4 position of 1,8-naphthalimides. The fluorescence properties of these derivatives can be changed by changing the nature of a substituent present on the aromatic ring [20]. Introduction of the substituents with different electron-donating capability, such as alkyl(aryl) amino [21], alkynyl/alkenyl [22,23], aryloxy or alkoxy groups [24] induces a polar CT excited state [4,5]. This ICT character leads to a large excited-state dipole and broad absorption and emission bands shifted at longer wavelengths.

2.1. 4-Aryl- and 4-aryloxy-substituted 1,8-naphthalimides

Diarylamine-substituted naphthalimide derivatives **1-3** and the similar compounds consisting of 2-naphthalene-1-yl-benzo[de]isoquinoline-1,3-dione (**4**, **5**) and bulky diphenylamine or naphthylphenylamine substituted as a side moieties were reported [25,26] (Fig. 1).

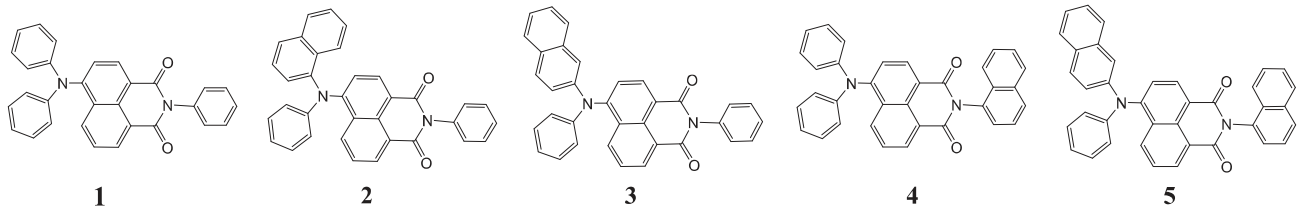

Fig. 1. Aryl- and 4-aryloxy-substituted naphthalimides.

It was found, that the glass transition temperature (T_g) increased in the order 72 ^oC (**1**) < 95 ^oC (**3**) < 105 ^oC (**2**). For compounds **4** and **5**, T_g were observed at 128 ^oC and 148 ^oC, respectively. Temperature of the onset of the thermal decomposition (T_{ID}) of **4** and **5** derivatives were at 368 ^oC and 407 ^oC, respectively. Increasing solvent polarity from *n*-hexane to dichloromethane (DCM) resulted in a 20 nm bathochromic shift of the maximum absorption wavelength (λ_{abs}) of compounds **1-3**. The commission Internationale de l'Eclairage (CIE) coordinates of the OLED device (ITO/DNTPD (60 nm)/NPD(20 nm)/Alq_3% dopant (20 nm)/Alq_3 (40 nm)/LiF/Al) were found to be (0.46, 0.52) for **4** and (0.48, 0.52) for **5** at 10 mA/cm^2. Luminance-efficiency were obtained 6.6 cd/A at the voltage of 5.9 V for OLED device containing **4** and 5.9 cd/A at the voltage of 6.3 V for OLED device containing **5**.

Wang and co-worker*s* [27] reported experimental and theoretical studies of similar naphthalimide compounds containing dimethylamino, diphenylamino groups (**6**, **7**), and different number of triphenylamino moieties (**8**, **9**, Fig. 2).

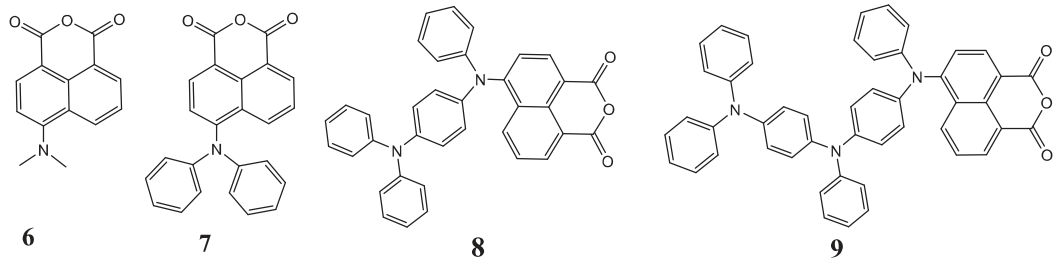

Fig. 2. Aryl- and 4-aryloxy-substituted naphthalimides.

The replacement of dimethylamino group at C4 position of naphthalic ring with diphenylamino group led to a 38 nm red-shift of λ_{abs} (cf. λ_{abs} of **6** and **7**). When the number of aromatic amino groups in compounds **8** and **9** increased to two and three, respectively, λ_{abs} of these compounds red shifted for 31 and 9 nm, respectively compared to **7**. Small red shifts of λ_{abs} of the solutions of compounds **6–9** in polar solvents were identified relative to those observed for the solutions in non-polar solvents. The fluorescence quantum yield (Φ_F) value of compound **7** (Φ_F = 0.057) was much smaller than that of compound **6** (Φ_F = 1) [28]. Φ_F of compounds **8** and **9** were very small (Φ_F = 0 and Φ_F = 0.01, respectively). The ionization potential values (IP_{CV}) increased for compounds **1-7 – 1-9** from 4.70 to 5.33 eV (Table 2.2). The structures of compounds **6–9** were optimized using hybrid density functional theory (B3LYP/6-31G(d)) method. It was established, that the naphthalic ring had a planar structure with a twisting angle of ~90° from the plane of directly connected amino group. IP_{CV} values increased along with the increase on the number of triphenylamino groups at C4 position and the optical band gap (E_g^{opt}) decreased following the order of **6** > **7** > **8** > **9**. The energy levels of HOMO-1 of compounds **6–9** increased along with the increase on the number of triphenylamino groups at 4-position.

Blue light-emitting naphthalimide derivatives containing electron-donating phenoxy or *t*-butyl modified phenoxy groups (**14**, **15)a-d**) were reported [29] (Fig. 3).

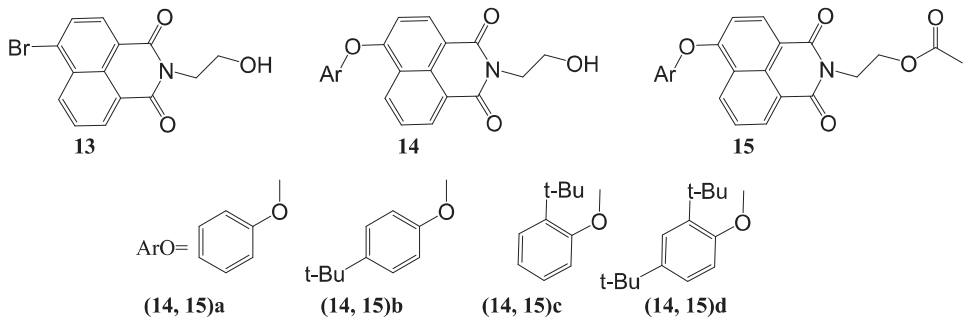

Fig. 3. Aryl- and 4-aryloxy-substituted naphthalimides.

Compounds **(14**, **15)d** showed red-shift compared to **13** in solution, due to that *t*-butyl acts as weak electron-donating substituent. The fluorescence properties of the solid films differed from those of the solutions due to the aggregation. The dilute solutions of compounds **(14**, **15)a** in chloroform showed blue fluorescence with high Φ_F of 0.55 and 0.82 respectively. The solid films of the derivatives (**14**, **15)a** showed bathochromic shift ($\Delta\lambda_{em}$ = 50 nm) with respect of those of the solutions. The films of compounds (**14**, **15)a** exhibited much lower Φ_F (<0.15) that those of compounds **(14**, **15)b** (0.27 and 0.46, repectively) [30]. Φ_F of the solutions of compounds **(14**, **15)c** were between 0.46–0.66, while those of the films were as low as 0.04. Derivatives (**14**, **15)d** had low EA_{CV} values ranging from -3.29 to -3.24 eV, and the IP_{CV} values ranging from 6.16 to 6.26 eV. Their electrochemical band gap (E_g^{elc}) were 2.92–3.01 eV, somewhat in good accordance with E_g^{opt} (3.03–3.08 eV).

2.2. 4-Ethynyl- and 4-ethenyl-substituted 1,8-naphthalimides

Donor-acceptor glass-forming derivatives (**16–18**) containing electron-accepting 1,8-naphthalimide moieties and electron-donating triphenylamino groups with ethynyl-containing linkages were obtained [31] (Fig. 4).

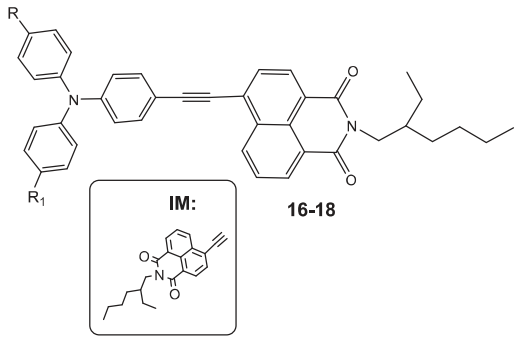

Comp.	R	R_1
16	H	H
17	H	IM
18	IM	IM

Fig. 4. 4-Ethynyl- and 4-ethenyl-substituted naphthalimides.

The glass-forming derivatives showed glass transition temperatures ranging from 73 to 96 °C, and the thermal stability with the temperature of the onset of thermal degradation ranged from 421 to 462 °C. Dilute solutions of the derivatives in chloroform exhibited emission quantum yields from 0.041 to 0.51 before deoxygenation and from 0.054 to 0.96 after deoxygenation with larger efficiency for compounds containing one (**16**) or two (**17**) 1,8-naphthalimide moieties. This observation was explained by the efficient delayed fluorescence in turn due to small singlet-triplet energy splittings. The presence of delayed fluorescence is supported by the time resolved fluorescence spectroscopy data. Time-of-flight technique revealed hole mobility exceeding 10^{-2} $cm^2 \cdot V^{-1} \cdot s^{-1}$ in the layer of **17**. Cyclic voltammetry measurements revealed close values of the solid state ionization potentials ranging from 5.48 to 5.61 eV and electron affinities ranging from -3.29 to -3.16 eV. The layer of **17** exhibited effective charge-transport with hole drift mobilities exceeding 10^{-2} $cm^2/V \cdot s$ (Table 1).

Table 1. Thermal, optical, photoelectrical and electrochemical characteristics of 1,8-naphthalimide derivatives.

Compound	T_g [°C]	T_m [°C]	T_{ID} [°C]	λ_{em}/ nm (Φ_F)	IP_{CV}, (eV)	EA_{CV}, (eV)	Mobility (μ_h), cm^2/V s
16	73	181	421	554 (0.17)	5.56	-3.18	10^{-3}
17	89	207	454	576 (0.25)	5.48	-3.16	10^{-2}
18	96	216	462	549 (0.011)	5.61	-3.29	-

T_g – glass-transition temperature; T_m – melting transition temperature; T_{ID} – temperature of the thermal decomposition; λ_{em} – maximum emission wavelength in solid films; Φ_F – fluorescence quantum yield in solid films; IP_{CV} – ionization potential; EA_{CV} – electron affinity; μ_h - hole mobility value at high electric fields.

Candidate for red OLEDs, starbust tris(4-(2-(*N*-butyl-1,8-naphthalimide)ethynyl)-phenyl)amine (**19**) showed a high fluorescence quantum yield in both dilute THF solution and 10 wt% doped poly(*N*-vinylcarbazole) thin film (Φ_F = 1.0) [32] (Fig. 2.8). A high brightness (6600 cd/m^2) and a high current efficiency (4.57 cd/A (at 420 cd/m^2)) with CIE (0.59, 0.40) were achieved at a relatively high doping concentration (20 wt%) in a **19**-based OLED.

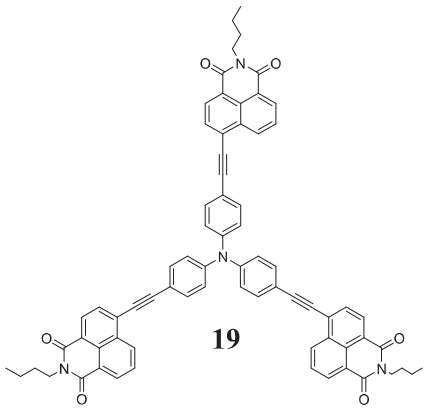

Fig. 5. 4-Ethynyl-substituted naphthalimide.

Solution-processable donor-acceptor molecules consisting of triphenylamine core and 1,8-naphthalimide arms were reported [33] (Fig. 6).

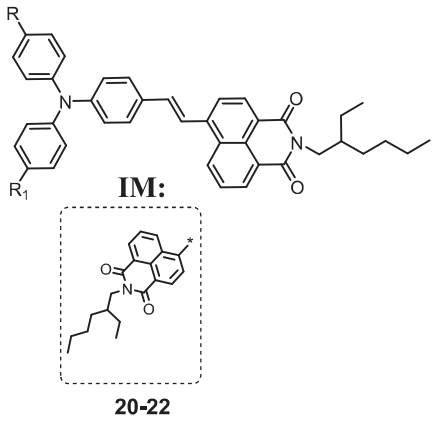

Comp.	**R**	**R$_1$**
20	H	H
21	H	CH=CH-**IM**
22	CH=CH-**IM**	CH=CH-**IM**

Fig. 6. 4-Ethynyl- and 4-ethenyl-substituted naphthalimides.

The synthesized molecules exhibit high thermal stability with the thermal degradation onset temperatures ranging from 431 to 448 °C. Besides, the compounds form glasses with glass-transition temperatures of 55 – 107 °C. Fluorescence quantum yields of of the solid samples are in the range of 0.09 – 0.18. The frontier orbital energies for the three synthesized compounds are similar and practically do not depend on the number of 1,8-naphthalimide moieties. Ionization potentials of the solid samples (5.75 – 5.80 eV) are comparable. The charge-transporting properties of the synthesized materials were studied using xerographic time-of-flight method. Hole mobilities in the layers of the compounds having one and two 1,8-naphthalimide moieties exceed 10^{-3} $cm^2 \cdot V^{-1} \cdot s^{-1}$ at high electric fields at room temperature (Table 2).

Table 2. Thermal, optical, photoelectrical and electrochemical characteristics of 1,8-naphthalimide derivatives.

Molecule	T_g [°C][a] (2nd heating)	T_{ID} [°C]	Film [nm]	λ_{em}	Φ_F film	I_p [eV]	Mobility (μ_h), $cm^2/V\ s$
20	55	431	624		0.18	5.75	10^{-3}
21	90	445	643		0.14	5.78	10^{-3}
22	107	448	652		0.09	5.80	10^{-4}

T_g – glass-transition temperature; T_{ID} – temperature of the onset of the thermal decomposition; λ_{em} – maximum emission wavelength in solid films; Φ_F – fluorescence quantum yield in solid films; I_p – ionization potential; μ_h - hole mobility value at high electric fields.

Two compounds with the donor-acceptor structure **23** and **24** for memory devices were described [33,34] (Fig. 7).

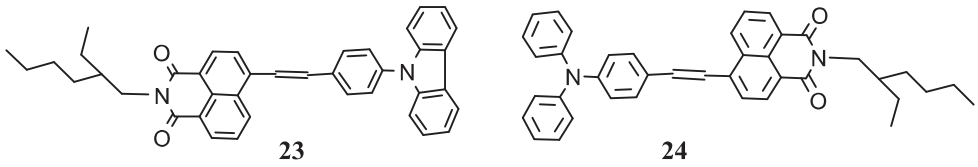

Fig. 7. 4-Ethynyl- and 4-ethenyl-substituted naphthalimides.

Both compounds exhibited high thermal stability with T_{ID} of 323 °C (for **23**) and 407 °C (for **24**). E_g^{opt} of the films of compounds **23** and **24** was 2.51 and 2.19 eV, respectively. IP_{CV} and EA_{CV} values were determined to be 5.66 eV (or 5.22 eV) and –3.15 eV (or –2.54 eV) for the **23** (or **24**). The memory device based on **23** exhibited much better characteristics than that based on **24** due to the presence of rigid carbazole moiety in favor of improving the surface morphology, which was revealed by atomic force microscopy measurement.

Two donor-acceptor type molecules consisting of triphenylamine and 1,8-naphthalimide moieties with the olefinic linkages between chromophores were synthesized [35] (**25, 26**) (Fig. 8).

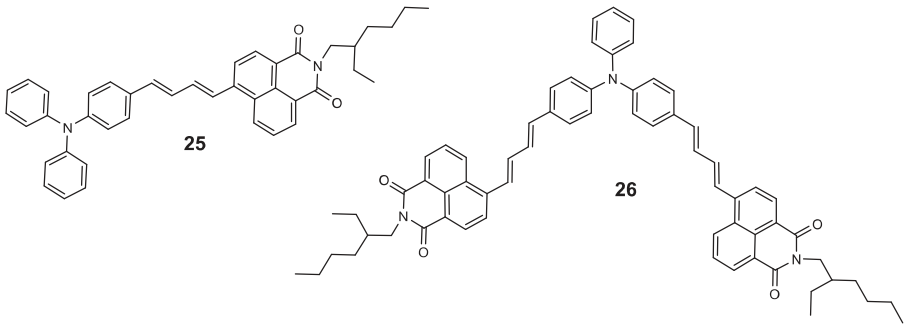

Fig. 8. 4-Ethynyl- and 4-ethenyl-substituted naphthalimides.

The compounds obtained are capable to form molecular glasses with glass transition temperatures of 54 °C and 75 °C recorded for mono substituted and di substituted derivatives of triphenylamine respectively. They exhibit high thermal stabilities with 5% weight loss temperatures of 350 °C and 363 °C. Fluorescence quantum yields of the dilute solutions of the synthesized compounds range from 0.065 to 0.72 while those of the solid films are 0.028 and 0.034. Due to pronounced electron donor-acceptor

character, the compounds showed solvatochromic red shifts of fluorescence up to 158 nm with significant reduction of the emission yield. Cyclic voltammetry measurements revealed close values of the solid state ionization potentials (5.22 eV and 5.27 eV) and of electron affinities (-3.20 eV and -3.18 eV). For the layer of the monosubstituted derivative of triphenylamine core hole mobility was found to be 2×10^{-3} cm^2 V^{-1} s^{-1} at an electric field of 6.1×10^5 Vcm^{-1} (Table 3).

Table 3. Thermal, optical, photoelectrical and electrochemical characteristics of 1,8-naphthalimide derivatives.

Compound	T_g [°C]	T_{ID} [°C]	λ_{em} / nm (Φ_F)	IP_{CV} (eV)[(b)]	EA_{CV} (eV)[(b)]	μ_h (cm^2/Vs)
25	54	350	640 (0.034)	5.25	-3.20	2×10^{-3}
26	75	363	644 (0.028)	5.22	-3.18	2.16×10^{-4}

T_g – glass-transition temperature; T_{ID} – temperature of the onset of the thermal decomposition; λ_{em} – maximum emission wavelength in solid films; Φ_F – fluorescence quantum yield in solid films; IP_{CV} – ionization potential; EA_{CV} – electron affinity; μ_h - hole mobility value at high electric fields.

Mikroyannidis and co-workers [36] reported two linear divinylenes **27** and **28** that contained fluorene and phenylene, as central unit and naphthalimide moieties as the terminal groups (Fig. 9).

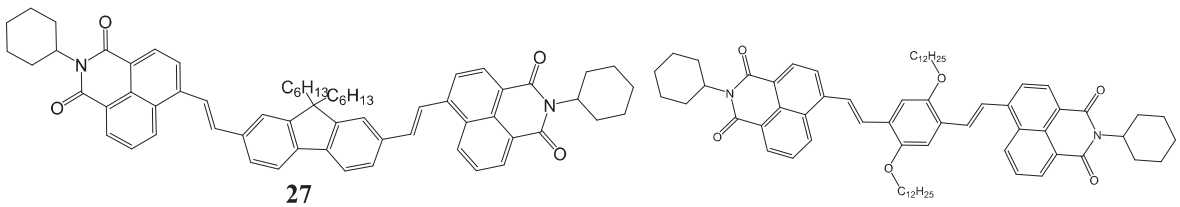

27 **28**

Fig. 9. 4-Ethynyl- and 4-ethenyl-substituted naphthalimides.

The values of T_{ID} **27** and **28** were 362 and 410 °C, respectively, and T_g followed the trend **27** (45 °C) > **28** (42 °C). E_g^{opt} values of **27** (2.55 eV) and **28** (2.48 eV) were comparable with that of poly(9,9-dioctylfluorene-2,7-vinylene) [37] (2.6 eV) and higher than that of poly(1-methoxy-4-(2-ethyl-hexyloxy)-*p*-phenylenevinylene) (MEH-PPV) (2.21 eV). **27**, **28** showed close Φ_F values (0.10–0.15). IP_{CV} values were 5.37 and 5.54 eV, and EA_{CV} values were –2.89 and –2.99 eV, respectively. Double-layer electroluminescent devices with the configuration of ITO/PEDOT:PSS (30 nm)/PVK:(25%)emitter (75 nm)/TPBI (25 nm)/LiF (0.5 nm)/Al (200 nm) were fabricated. The devices based on **27** and **28** showed the similar current efficiency of 0.15–0.10 cd/A. For the device based on **27**, the maximum luminance of 143 cd/m^2 are comparable to that of 124 cd/m^2 based on **28**.

Green host compounds (**29–31**) containing the naphthalimide moieties were reported [38] (Fig. 10).

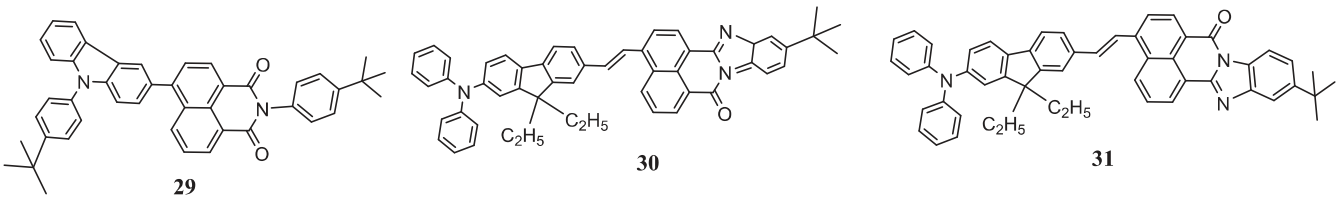

Fig. 10. 4-Ethynyl- and 4-ethenyl-substituted naphthalimides.

λ_{abs} of dilute DCM solution of compound **30** was red-shifted by 10 nm compared with the absorption spectra of the solution of compound **31**. Both compounds exhibited high T_{ID} (higher than 400 °C). T_g of the two compounds was not identified, however high melting points (>290 °C) were observed. IP_{CV} values of **29** and **31** were calculated to be 5.38 eV and 5.67 eV, respectively. EA_{CV} values of –3.14 eV and –2.99 eV were deduced for **29** and **31**, respectively. OLEDs employing **29**/**31** as the guest/host pair were fabricated. Devices I and II represented OLEDs with **31** blending ratio of 3 wt% and 6 wt%, respectively. The turn-on voltages of device I and II were 5.2 and 4.1 V, respectively. Device II showed higher current at the similar driving voltages (< 13 V) relative to device I.

2.3. 1,8-Naphthalimide moiety containing hydrazones and Schiff bases

Gan and co-workers [39] reported naphthalimide derivatives (**32-38**) containing Schiff base moiety (Fig. 11).

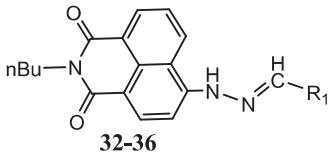

32-36

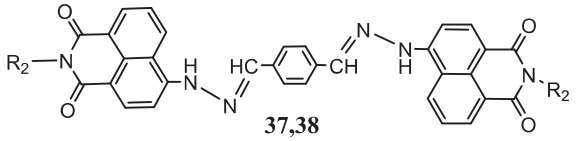

37,38

Comp.	32	33	34	35	36	37	38
$\mathbf{R_1}$	$-CH_3$	-phenyl	4-methoxyphenyl	-anthracenyl	4-dimethylaminophenyl	–	–
$\mathbf{R_2}$	–	–	–	–	–	*n*-butyl	*n*-$C_{12}H_{25}$

Fig. 11. Naphthalimide moiety containing hydrazones.

By extending the conjugation length, the fluorescent lifetimes of the solutions of **33** and **36** in tetrahydrofuran (THF) decreased to 4.71 and 0.29 ns, respectively, in comparison with that of **33** (7.4 ns). The similar trend was evident for compounds **34** and **36**. λ_{abs} of **33–38** in acetonitrile were red-shifted by 10, 22, 33, 46, 54, and 55 nm, respectively with respect of that of **32**. λ_{em} of the solid films of compounds **32–38** were shifted to longer wavelengths with respect of that of **33**. The emission of the film of compound **36** showed a red-shift of more than 110 nm compared to that of **32**. IP_{CV} values of naphthalimides **33**–**38** were in the range of 6.9–7.3 eV. OLEDs were prepared. The device with a 45 nm thick **36** film had maximum luminance of 15.5 cd/m^2 and a maximum current density of 2.9 mA/cm^2 at an applied voltage of 22 V. Turn-on voltage of this EL device was 14 V. In the same device structure, the organic photovoltaic properties containing **36** with a 1.1 V voltage and a 5 μA/cm^2 current density were observed, when the device was irradiated by the quartz light at 50 W.

Hydrazones containing electron-accepting 1,8-naphthalimide species and electron-donating triphenylamino moieties (Fig. 12) were reported (**39-42**) [40].

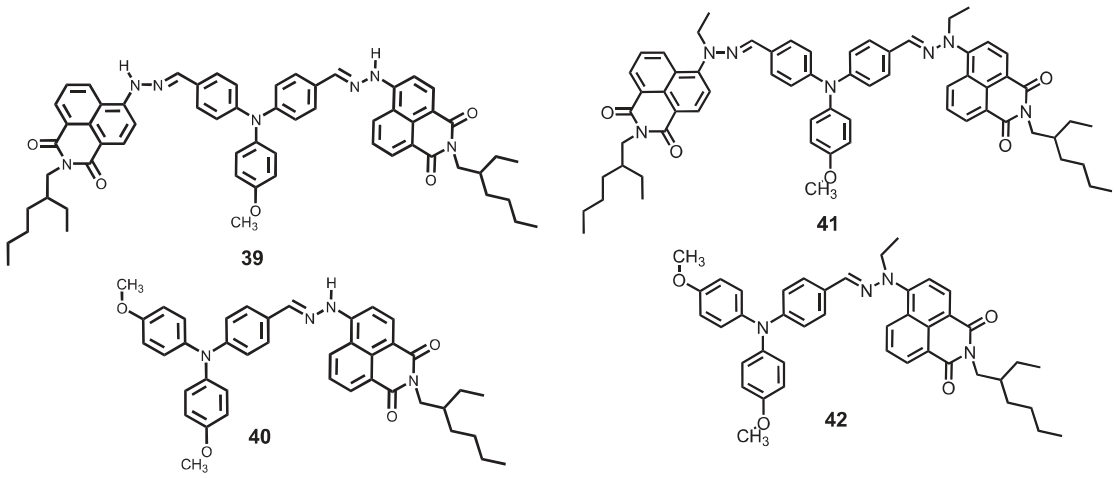

Fig. 12. Naphthalimide moiety containing hydrazones.

The hydrazones exhibit initial mass loss temperatures in the range of 268-348 ^{o}C. It was found, that alkyl-substituted derivatives **41** and **42** exhibit lower thermal stability than the corresponding unsubstituted compounds (**39** and **40**). They can form glasses with glass transition temperatures in the range of 46-142 ^{o}C. The presence of electron-accepting 1,8-naphthalimide species has minor effect on the ionization potentials of these compounds. The layers of the solid solutions of compounds **41** and **42** in PC-Z (50%) showed mh exceeding 10^{-5} cm^2 V^{-1} s^{-1} at high electric fields at 25 ^{o}C. The ionization potentials of the alkyl-substituted compounds, measured by electron photoemission technique are 5.45 eV (Table 4).

Table 4. Thermal, optical, photoelectrical and electrochemical characteristics of 1,8-naphthalimide derivatives.

Material	$T_{ID,}$ (^{o}C)	$T_{g,}$ (^{o}C)	$IP_{CV,}$ (eV)	$EA_{CV,}$ (eV)	E_g^{opt}, (eV)	E_g^{elc}, (eV)

39	275	142	5.06	-2.91	2.27	2.15
40	348	87	5.01	-2.91	2.27	2.10
41	268	73	5.06	-3	2.24	2.06
42	303	46	5.01	-3	2.25	2.01

T_g – glass-transition temperature; T_{ID} – decomposition temperature, IP_{CV} – ionization potential; EA_{CV} – electron affinity; E_g^{elc} – electrochemical band gap; E_g^{opt} – optical band gap.

2.4. 4-(Heter)oaromatic-substituted 1,8-naphthalimides

A series of starburst benzene-based glass-forming molecules (**43a-e**) with terminal naphthalimide moieties for optoelectronic devices were reported [41] (Fig. 13).

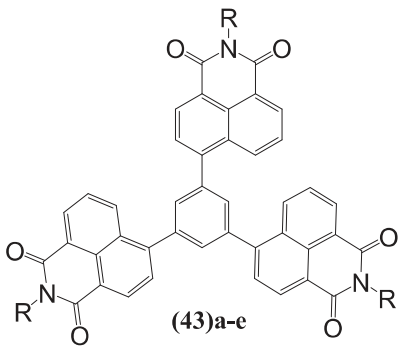

43a, R= *n*-butyl
43b, R= *n*-hexyl
43c, R= 2-ethylhexyl
43d, R= 3,5-dimethylphenyl
43e, R= 9,9-dibuylfluorophenyl-2-yl

Fig. 13. 4-(Heter)oaromatic-substituted naphthalimides.

Glass transitions were observed for all compounds (**43a-e**). T_g reached as high as 254 °C for compound **43d** and 193 °C for **43e**. The compounds with more rigid moieties (**43d** and **43e**) exhibited higher T_g than those with flexible alkyl substituents (**43a-e**). Thermogravimetric analysis (TGA) experiments revealed that all these compounds exhibited high thermal stability with T_{ID} up to 489 °C. Two organic electroluminescent (EL) devices ITO/MoO_3 (3 nm)/NPB (40 nm)/Alq_3 (20 nm)/Bphen (20 nm)/electron transporter (20 nm)/Cs_2CO_3 (1 nm)/Al (100 nm) were fabricated, where **43a** and tris(8-

hydroxyquinoline)aluminium (Alq_3) were chosen as electron transporter. The **43a** based device showed the current density of 48.7 mA/cm^2, luminance of 985 cd/m^2 at 5 V, compared with 1 mA/cm^2 and 23 cd/m^2 observed for the Alq_3-based device.

Another series of star-shaped small molecules **44**–**47** with a TPA core and peripheral 1,8-naphthalimide groups were synthesized by direct arylation [42] (Fig. 14).

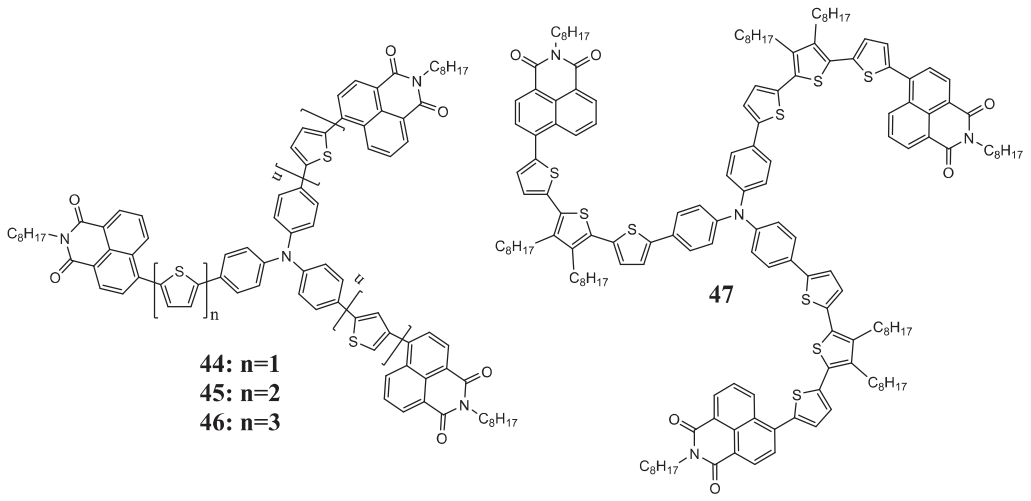

Fig. 14. 4-(Heter)oaromatic-substituted naphthalimides.

TGA investigations revealed that these molecules are of very good thermal stability with the 5% decomposition temperature up to 480, Bulk heterojunction (BHJ) organic solar cells (OSCs) with a device structure of ITO/ PEDOT:PSS/**44**–**47**:PC71BM/LiF/Al were fabricated. All OSCs devices gave the EQE maxima at 475 nm, which are 28.6% for **44**, 38.5% for **45**, 42.0% for **46**, and 44.5% for **47**. BHJ OSCs with **48**:PC71BM blend as the active layer gave a PCE of 2.32% and a high V_{OC} of 0.94 V. This preliminary result demonstrates that 1,8-naphthalimide based star-shaped molecules are promising donor materials for OSCs. Hole mobility of **44, 45, 46** and **47** reached $1.04 \cdot 10^{-5}$, $6.70 \cdot 10^{-5}$, $2.49 \cdot 10^{-5}$, and $7.20 \cdot 10^{-5}$ cm^{2}V^{-1} s^{-1}, respectively.

Two types of EL devices were fabricated using bipolar compounds based on naphthalimide moietys (**48**–**53** and **54**–**56**) [19] (Fig. 15).

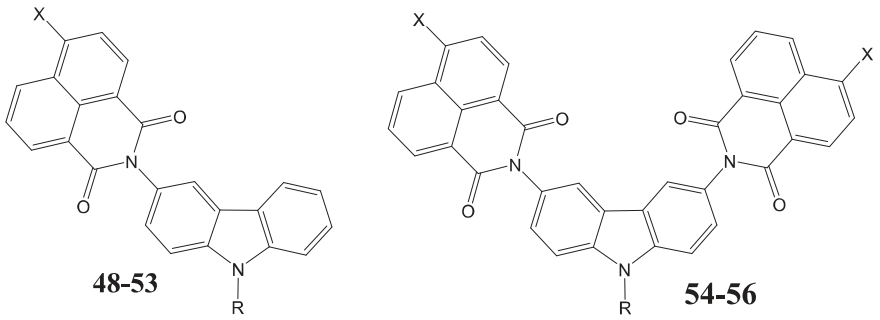

48, X=piperidino, R= C_2H_5
49, X= piperidino, R= C_6H_{13}
50, X=piperidino, R= $CH_2C_6H_5$
51, X=$N(CH_3)_2$, R= C_2H_5
52, X= $N(CH_3)_2$, R= C_6H_{13}
53, X= $N(CH_3)_2$, R= $CH_2C_6H_5$

54, X= piperidino, R= C_2H_5
55, X= piperidino, R= $CH_2C_6H_5$
56, X= $N(CH_3)_2$, R= C_2H_5

Fig. 15. 4-(Heter)oaromatic-substituted naphthalimides.

Device 1 had an architecture: ITO/compounds **48–53** or **54–56** (50–100 nm)/LiF (1 nm)/AlLi. Device 2 had the following structure: ITO/CuPc (10 nm)/TPD (10 nm)/compound **51** (30 nm)/$BePP_2$ (45 nm)/LiF (1 nm)/AlLi. The device 2 had maximum brightness of 110 cd/m^2 at a driving voltage of 21 V and a maximum current density of 240 mA/cm^2. From the synthesized compounds **54–56** single-layer devices were prepared (ITO/**54–56** (50–100 nm)/LiF (1 nm)/AlLi). The devices containing triads (**54–56**) displayed higher brightness, lower turn-on voltage than those containing **48–53**. Due to improve the device efficiency the device 2 with additional electron-transporting layer (bis[2-(2-hydroxyphenyl)-pyridine]beryllium ($BePP_2$)) and hole-transporting layer (copper(II)phthalocyanine (CuPc) and *N,N'*-diphenyl-*N,N'*-bis(3-methylphenyl)-(1,1'-biphenyl)-4,4'-diamine (TPD)) were prepared. The maximum brightness of the device 2 reached 4800 cd/m^2 at the driving voltage of 21 V, the maximum current density increased up to 410 mA/cm^2.

Gudeika and co-workers [43,44] reported a donor-acceptor carbazole derivative (**54-62**) containing napthalimide moiety at C-4 position (Fig. 16) and its optical, photoelectrical and electrochemical data are summarized in Table 5.

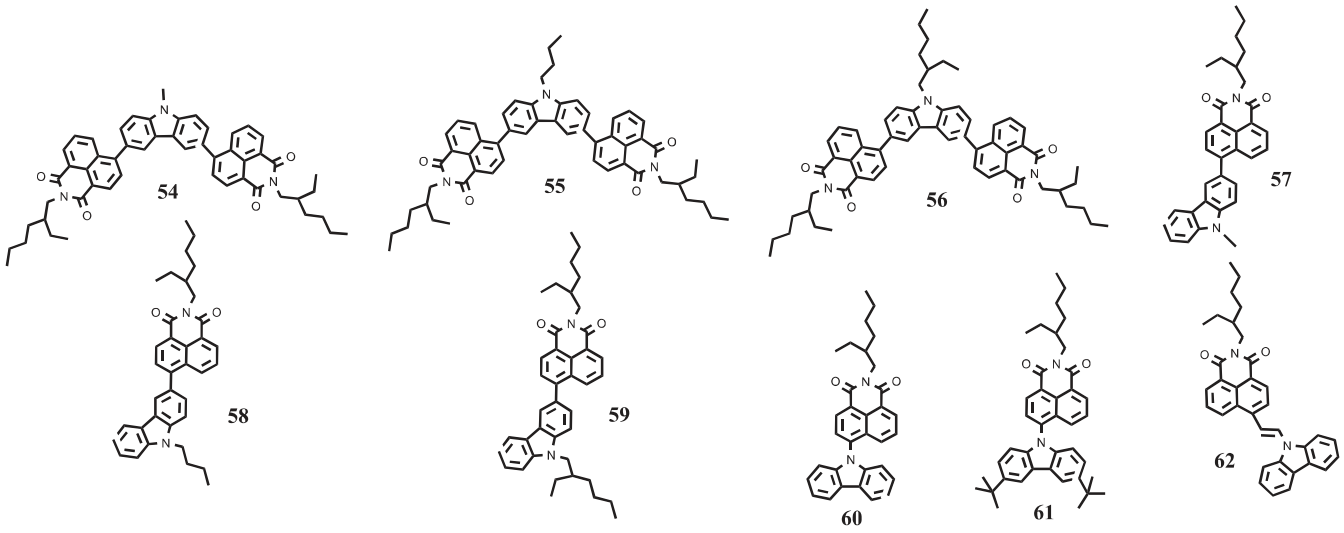

Fig. 16. 4-(Heter)oaromatic-substituted naphthalimides.

Compounds **54-62** exhibit high thermal stability with 5% weight loss temperature up to 476 °C. Most of the synthesized compounds are capable of glass formation with glass transition temperatures from 30 to 87 °C. The cyclic voltammetry measurements showed that the solid state ionization potentials values of the carbazole and 1,8-naphthalimide derivatives range from 5.46 to 5.76 eV and the electron affinities values range from -3.04 to -2.92 eV. The 3- and 3,6-naphthalimide-substituted derivatives of carbazole in the solid state were found to emit in the green region with quantum yields ranging from 0.01 to 0.45. The studied derivatives of carbazole and 1,8-naphthalimide display hole mobility values of the order of 10^{-6} cm^2/Vs at the electric fields in the range from $(3.6\text{-}8.1)\times10^5$ V/cm (Table 5).

Table 5. Thermal, optical, photoelectrical and electrochemical characteristics of carbazole derivative containing napthalimide moiety.

Material	$T_{g,}$ (°C)	$T_{ID,}$ (°C)	$\lambda_{em,}$ (nm)	Φ_F	$IP_{CV,}$ (eV)	$EA_{CV,}$ (eV)	Mobility (μ_h), cm^2/V s
54	101	476	541	<0.01	5.68	-2.94	1.43×10^{-6}

55	96	457	522	0.17	5.67	-2.95	2.37×10^{-6}
56	30	383	513	0.06	5.75	-2.94	0.87×10^{-6}
57	47	434	522	0.01	5.56	-2.94	1.6×10^{-6}
58	15	385	533	0.07	5.55	-2.93	-
59	-5	351	519	0.06	5.58	-2.92	-
60	40	373	501	0.10	5.76	-3.04	3×10^{-6}
61	48	417	537	<0.01	5.46	-3.01	0.47×10^{-6}
62	-	422	563	0.45	5.45	-3.00	0.14×10^{-6}

T_g – glass-transition temperature; T_{ID} – temperature of the thermal decomposition; λ_{em} – maximum emission wavelength in solid films; Φ_F – fluorescence quantum yield in solid films; IP_{CV} – ionization potential; EA_{CV} – electron affinity; μ_h - hole mobility value of the order of 10^{-6} cm^2/Vs at the electric fields in the range from $(3.6\text{-}8.1)\times10^5$ V/cm.

Naphthalimide-substituted derivatives of fluorene containing different alkyl substituents (**63-68**) were reported [45] (Fig. 17).

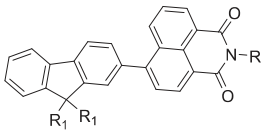

63-65

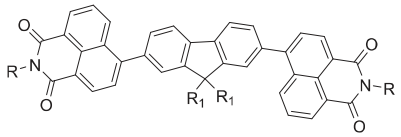

66-68

	R	R_1
63, 66	C_2H_5	$C_4H_9(C_2H_5)CHCH_2$
64, 67	$C_4H_9(C_2H_5)CHCH_2$	$C_4H_9(C_2H_5)CHCH_2$
65, 68	C_8H_{17}	C_8H_{17}

Fig. 17. 4-(Heter)oaromatic-substituted naphthalimides.

Most of the synthesized materials were found to constitute glasses with glass transition temperatures ranging from 30 to 76 ^{o}C. Their initial weight loss temperatures range from 315 to 466 ^{o}C. The naphthalimide-substituted derivatives of fluorene in the solid state fluorescence quantum yields were found to be in the range of 0.06-0.25. Time of-flight electron drift mobilities of the layer of **68** in air approach 1.2×10^{-3} cm^2 V^{-1}s^{-1} at an eletric field of 6.4×10^5 Vcm^{-1} (Table 6).

Table 6. Thermal, optical, photoelectrical and electrochemical characteristics of carbazole derivative containing napthalimide moiety.

Material	$T_{g,}$ (^{o}C)	$T_{ID,}$ (^{o}C)	$\lambda_{em,}$ (nm)	Φ_F	Mobility (μ_e), cm^2/V s
63	30	392	474	0.23	3.8×10^{-5} (6.4×10^{-5} V/cm^{-1})
64	50	304	495	0.17	10^{-5} (6.4×10^{-5} V/cm^{-1})
65	-19	290	477	0.25	-
66	76	457	489	0.14	-
67	49	422	469	0.07	4×10^{-4} (6.4×10^{-5} V/cm^{-1})
68	59	441	480	0.25	1.2×10^{-3} (6.4×10^{-5} V/cm^{-1})

T_g – glass-transition temperature; T_{ID} – temperature of the onset of the thermal decomposition; λ_{em} – maximum emission wavelength in solid films; Φ_F – fluorescence quantum yield in solid films; μ_e - electron mobility value.

Four new derivatives of triphenylamine containing different number of naphthalimide moieties (**69-72**) were synthesized [46] (Fig. 18).

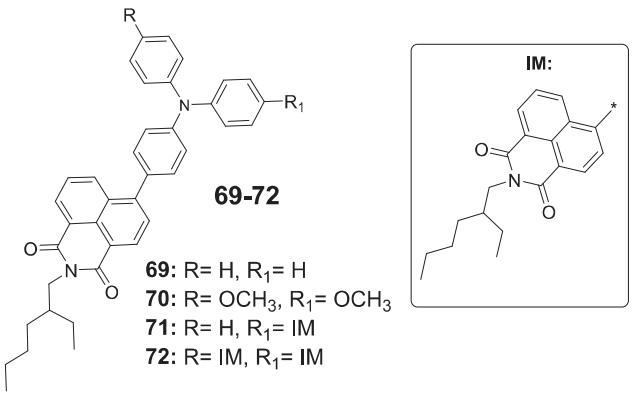

Fig. 18. 4-(Heter)oaromatic-substituted naphthalimides.

The compounds obtained are capable to form molecular glasses with glass transition temperatures ranging from 45 to 93 °C. They exhibit very high thermal stabilities with 5% weight loss temperatures ranging from 429 to 483 °C. The ionization potentials of the solid samples of the compounds established by electron photoemission spectrometry in air ranged from 5.57 to 6.01 eV. The lowest ionization potentials and the best charge-transporting properties were observed for the amorphous layers of 4-(4'-(di-(4''-methoxyphenyl)amino)phenyl)-*N*-(2-ethylhexyl)-1,8-naphthalimide (**70**). Electron mobilities of 7.5×10^{-4} $cm^2 \cdot V^{-1} \cdot s^{-1}$ and hole mobilities of 1.1×10^{-4} cm^2 $V^{-1} \cdot s^{-1}$ were recorded for this compound at an electric field of 1×10^6 V/cm. Compounds containing no methoxy groups exhibit electron mobilities by 2-3 order of magnitude higher than the hole mobilities. The comparison between compounds **69** and **70** shows that the methoxy groups increase the hole mobility by ~3 orders of magnitude (Table 7).

Table 7. Thermal, optical, photoelectrical and electrochemical characteristics of carbazole derivative containing napthalimide moiety.

Material	T_g, (°C)	T_{ID}, (°C)	λ_{em}, (nm)	Φ_F	I_p, (eV)	Mobility (μ_h), cm^2/V s	Mobility (μ_e), cm^2/V s
69	47	437	557	0.11	5.79	$3.7\cdot10^{-7}$	2.3×10^{-4}

70	45	429	630	0.10	5.57	1.1×10^{-4}	7.5×10^{-4}
71	76	448	569	0.16	5.93	4×10^{-7}	4.7×10^{-5}
72	93	483	570	0.23	6.01	2×10^{-8}[a]	-

T_g – glass-transition temperature; T_{ID} – temperature of the onset of the thermal decomposition; λ_{em} – maximum emission wavelength in solid films; Φ_F – fluorescence quantum yield in solid films; I_p - ionization potential was established from electron photoemission in air spectra; Hole and electron drift mobility values at electric field 1×10^6 V/cm. [a] Hole drift mobility value at electric field 3.6×10^5 V/cm.

2.5. 1,8-Naphthalimide polymers with aromatic substituents at the 4-position

It was shown that when *N*-aryl-1,8-naphthalimide derivatives were incorporated into polymer chains, the resulting materials show interesting fluorescent and electroluminescent properties [47,48]. If *N*-arylnaphthalimide or 1,8-naphthoilenearylimidazole derivatives have different electron-accepting (or donating) groups and different coplanar degree of molecular structures, these groups can change the optical properties shift the fluorescence wavelengths, change the emission quantum yields [49]. By controlling the electron-donating property of the substituent at the C-4 position of 1,8-naphthalimide moiety, the emission color of the resulting polymer can be tunable within a large range. Moreover, highly efficient and nearly pure white electroluminescence can be achieved using such polymers.

Several green light emitting polyfluorenes containing *N*-arylnaphthalimide and 1,8-naphthoilenearyl-imidazole as end caps (**73–77)P** for optoelectronics were reported [50] (Fig. 19).

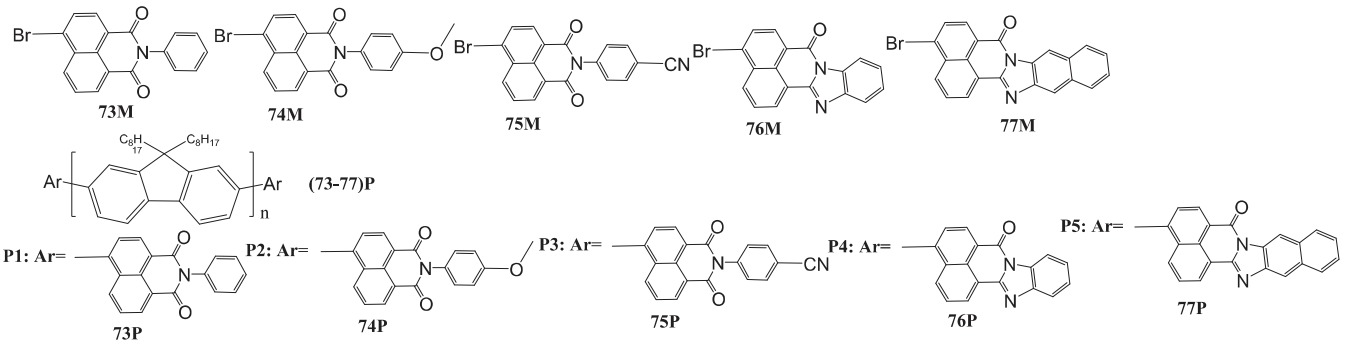

Fig. 19. 1,8-Naphthalimide polymers.

T_{ID} of the polymers ranged from 416 to 424 °C and T_g was in the range of 110–113 °C. Φ_F of compounds **(73-75)M** were in the range of 0.01–0.82. The energy levels of the polymers were in the range of 5.62–5.70 eV (for IP_{CV}), and -2.36 – -2.12 eV (for EA_{CV}), and these energy levels of the polymers had slightly different than those of polyfluorene [51]. The devices were fabricated in the configuration of ITO/PEDOT:PSS/PVK/emission layer/Ca/Ag. The turn-on voltage, maximum brightness, and maximum luminance of the devices contaning polymers were: (11 V, 930 cd/m^2, 0.19 cd/A) for the device containing **73P**, (10 V, 2890 cd/m^2, 0.28 cd/A) for the device with the emission layer of **74P**, (11 V, 772 cd/m^2, 0.15 cd/A) for the device with **75P**, (6 V, 11500 cd/m^2, 0.83 cd/A) for the device with **76P**, and (7 V, 6534 cd/m^2, 0.56 cd/A) for the device with **75P**. The devices based on **(73–75)P** had higher turn-on voltages and lower current density. The device with **76P** emitted pure green light, and exhibited maximum brightness of 11500 cd/m^2 at 12 V (Table 8).

Table 8. Properties of 1,8-naphthalimide derivatives.

Material	$T_{ID,}$ (°C)	$T_{g,}$ (°C)	$IP_{CV,}$ (eV)	$EA_{CV,}$ (eV)	Turn-on voltage, (V)	Brightness max, (cd/m^2)	Luminous efficiency max, (cd/A)
73	420	110	5.62	–2.14	22	930	0.19

74	424	112	5.67	–2.12	20	2890	0.28
75	421	110	5.68	–2.15	22	772	0.15
76	417	113	5.67	–2.24	6	11500	0.83
77	416	110	5.70	–2.36	7	6354	0.56

T_{ID} – temperature of the onset of the thermal decomposition; T_g – glass-transition temperature; IP_{CV} – ionization potential; EA_{CV} – electron affinity.

Tu and co-workers [52] reported copolymers (**78–83**) with naphthalimide chromophores chemically doped into the polyfluorene backbones (Fig. 20).

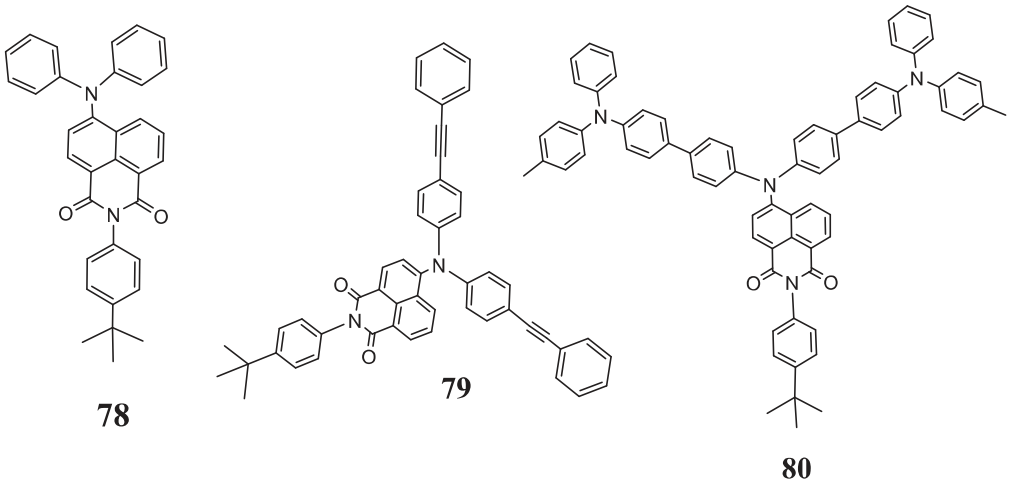

78

79

80

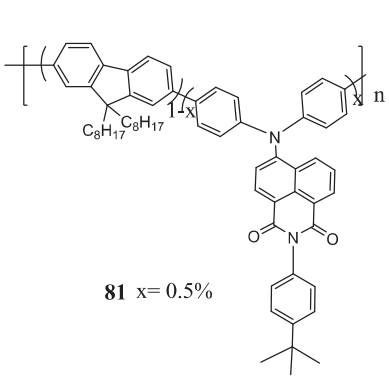

81 x= 0.5%

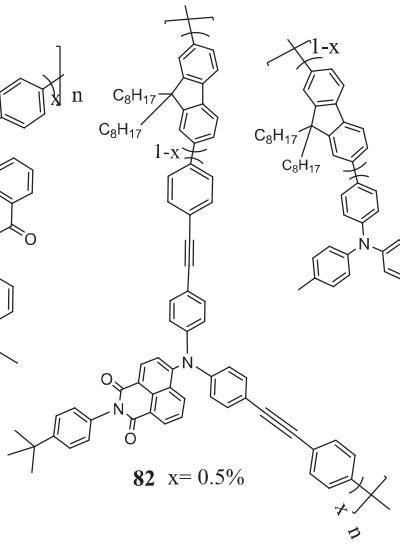

82 x= 0.5%

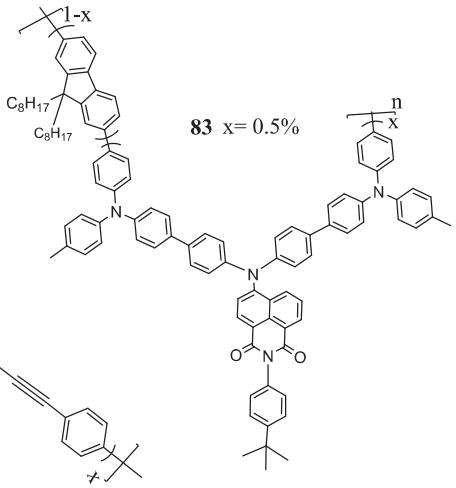

83 x= 0.5%

Fig. 20. 1,8-Naphthalimide polymers.

The films of the compounds **79**, **80** showed red fluorescence with Φ_F of 0.30 and 0.25, respectively. Their IP_{CV} and EA_{CV} values were determined to be (5.60 eV, –3.30 eV) for **78**, (5.24 eV, –3.26 eV) for **79**, and (5.26 eV, –3.31 eV) for **80**. The electroluminescent devices with a configuration of indium tin oxide (ITO)/(PEDOT; 50 nm)/copolymer(80 nm)/Ca(10 nm)/Al(100 nm) were fabricated by spin coating the polymer solution onto PEDOT-modified ITO glass under ambient conditions. The device made from **83** showed the best performance, with a maximum brightness of 11 900 cd/m^2, a luminance efficiency of 3.8 cd/A, a power efficiency of 2.0 lm/W, and external quantum efficiency of 1.50%. In the case of **83**, when a driving voltages of 8, 10, 12, and 14 V were applied the CIE coordinates under the different voltages were (0.32, 0.36), (0.32, 0.36), (0.31, 0.35), and (0.31, 0.35), respectively, corresponding to maximum brightnesses of 144, 997, 3026, and 5560 cd/m^2, respectively.

A series of highly efficient blue electroluminescent copolymers containing pendant naphthalimide species were reported [53] (Fig. 21).

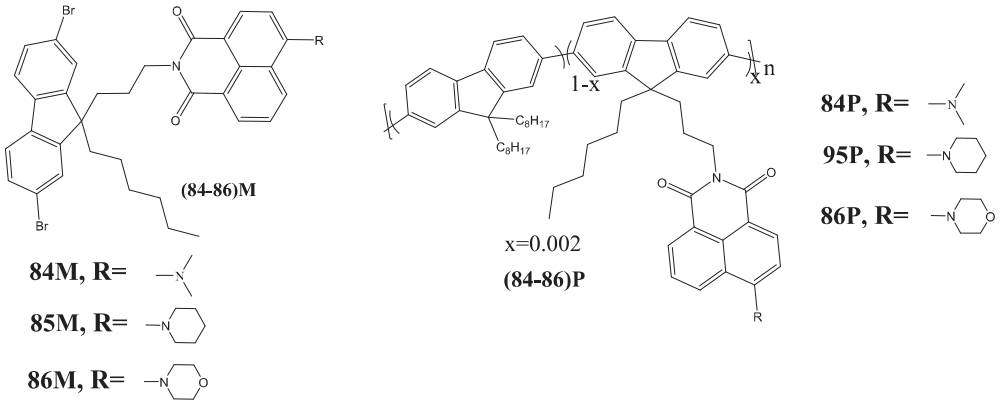

Fig. 21. 1,8-Naphthalimide polymers.

EA_{CV} and IP_{CV} values of polymers **84P**, **85P** and **86P** were estimated to be –2.12 eV and 5.80 eV, respectively. FL spectrum of **85M** was red shifted by 5 nm relative to those of **84M** and **86M**. The

toluene solutions of all three copolymers exhibited high Φ_F values (0.74–0.91). Single-layer electroluminescent devices were fabricated with the configuration of ITO/(PEDOT:PSS) (40 nm)/copolymer (90 nm)/Ca (10 nm)/Al (100 nm). The devices containing the layers of **84P**, **85P** and **86P** exhibited turn on voltages of 3.5 V, luminous efficiencies of 2.20–5.22 cd/A and power efficiency of 1.53–3.28 lm/W.

Wang *et al.* [51] developed several series of copolymers with pendant 1,8-naphthalimide moieties (**87**–**89**) for single-layer white OLEDs (Fig. 22).

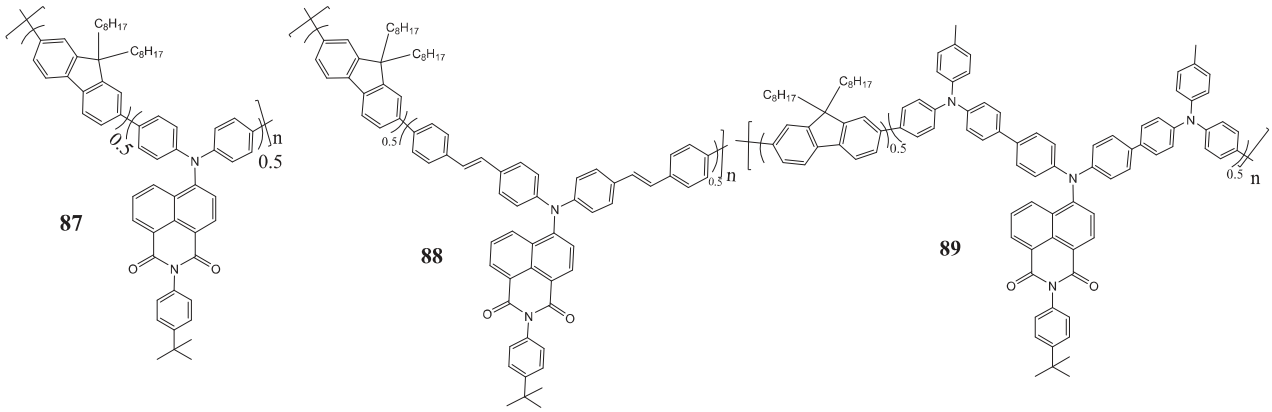

Fig. 22. 1,8-Naphthalimide polymers.

Among **87**–**89** the best performance with a maximum luminance of 11 900 cd/m^2, a peak external quantum efficiency of 1.5%, a luminance efficiency of 3.8 cd/A, and a power efficiency of 2.0 lm/W in the device configuration of ITO/PEDOT:PSS (50 nm)/**89** (80 nm)/Ca (10 nm)/Al (100 nm) showed **89**. In the voltage range corresponding to the maximum brightness from 144 cd/m^2 to 5560 cd/m^2, the CIE coordinates remained relatively stable ($\Delta x = 0.01$, $\Delta y = 0.01$) with CIE (0.32, 0.36) at 8 V and (0.31, 0.35) at 14 V.

Another series of white light-emitting copolymers (**90**, **91**) with pendant naphthalymide moieties also were reported [54,55] (Fig. 23).

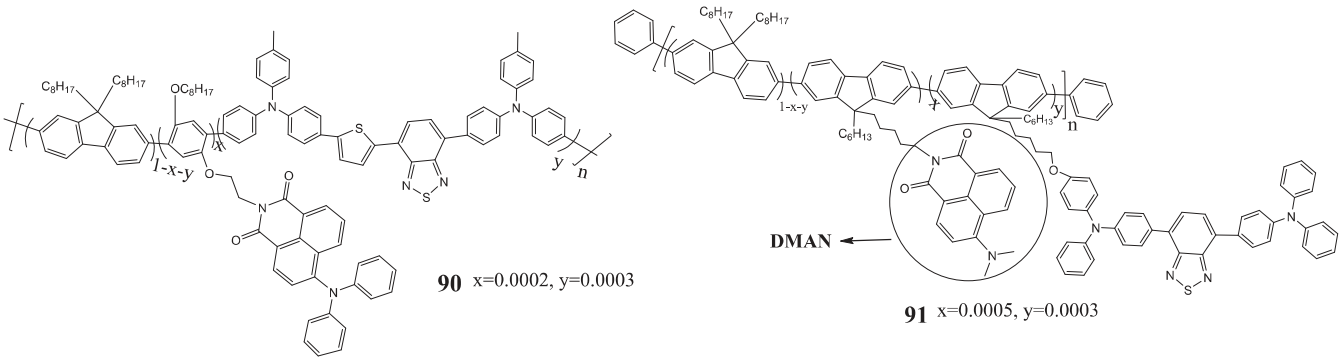

Fig. 23. 1,8-Naphthalimide polymers.

Although the device based on **90** could not give attractive EL efficiencies (luminance efficiency of 1.59 cd/A and power efficiency of 0.83 lm/W), it showed very good white light color quality with CIE coordinates at (0.31, 0.34) and stable EL spectra from 8 V to 12 V. White-emitting terpolymer **91** with bluish-green emitting chromophore 4-dimethylamino-1,8-naphthalimide (DMAN) OLED with the configuration of ITO/PEDOT:PSS (40 nm)/copolymer (90 nm)/Ca (10 nm)/Al (100 nm) showed EL with luminance efficiency of 12.8 cd/A, external quantum efficiency of 5.4% and power efficiency of 8.5 lm/W. OLED with **91** emitted white light of high quality with CIE coordinates of (0.31, 0.36) and nearly invariant EL spectra from 6 V to 10 V.

Lee and co-workers [56] reported low-band-gap copolymer of fluorene and diphenylamine with the derivatives of naphthalimide as the pendants and the end caps (**92**, Fig. 24).

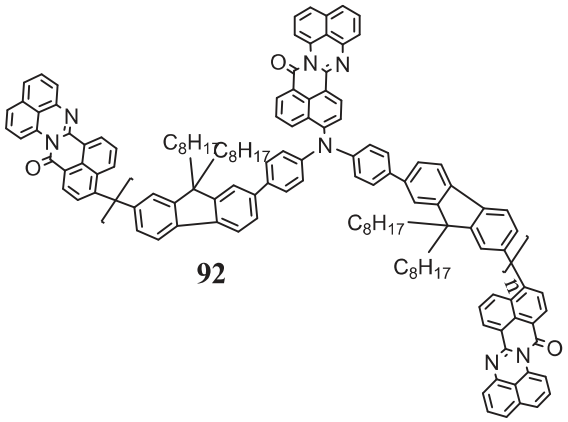

92

Fig. 24. 1,8-Naphthalimide polymer.

T_{ID} of **92** was observed at 423 °C and E_g^{opt} of **92** was found to be 1.82 eV. IP_{CV} and EA_{CV} values of **92** were 5.21 and –3.32 eV, respectively. E_g^{elc} of **92** was 1.89 eV, and E_g^{elc} was larger than E_g^{opt} (1.82 eV), due to the interface barrier for charge injection [57]. The bulk heterojunction solar cell were fabricated with a structure of ITO/PEDOT:PSS (50 nm)/9**2**:PCBM (110 nm)/LiF (0.5 nm)/Al (80 nm). The power conversion efficiencies of solar cells based on **92**:PCBM (1:3) and **92**:PCBM (1:4) were 0.61% and 0.67%, respectively, under the illumination of AM1.5 G, 100 mW/cm^2. The solar cell fabricated from **92**:PCBM (1:4) exhibited open-circuit voltage (0.55 V) and a higher short-circuit current (4.46 mA/cm^2), which resulted in a higher power conversion efficiencies of 0.67%. The maximum external quantum efficiency value of **92**/PCBM (1:4) device was 30.9% at 535 nm.

2.6. 1,8-Naphthalimide dendrimers with aromatic substituents at the 4-position

Dendrimers provide new opportunities for precisely placing some charge-carrier transporting units by the generation in a three-dimensional nanoscale construction. In contrast to polymers, the size and architecture of dendrimers can be specifically controlled in their synthesis. The dendritic architecture can be also used to improve the solubility of organic electroactive compounds to form uniform films by solution processing, thus overcoming the high cost of the vacuum deposition process.

The design and modification of the Polyamidoamines (PAMAMs) dendrimers with fluorescent 1,8-naphthalimide units could produce new interesting optical and photophysical properties.

The same group reported several dendrimers whose periphery was modified with naphthalimide moieties having different substituents at C-4 position (**93–96**) [58,59] (Fig. 25).

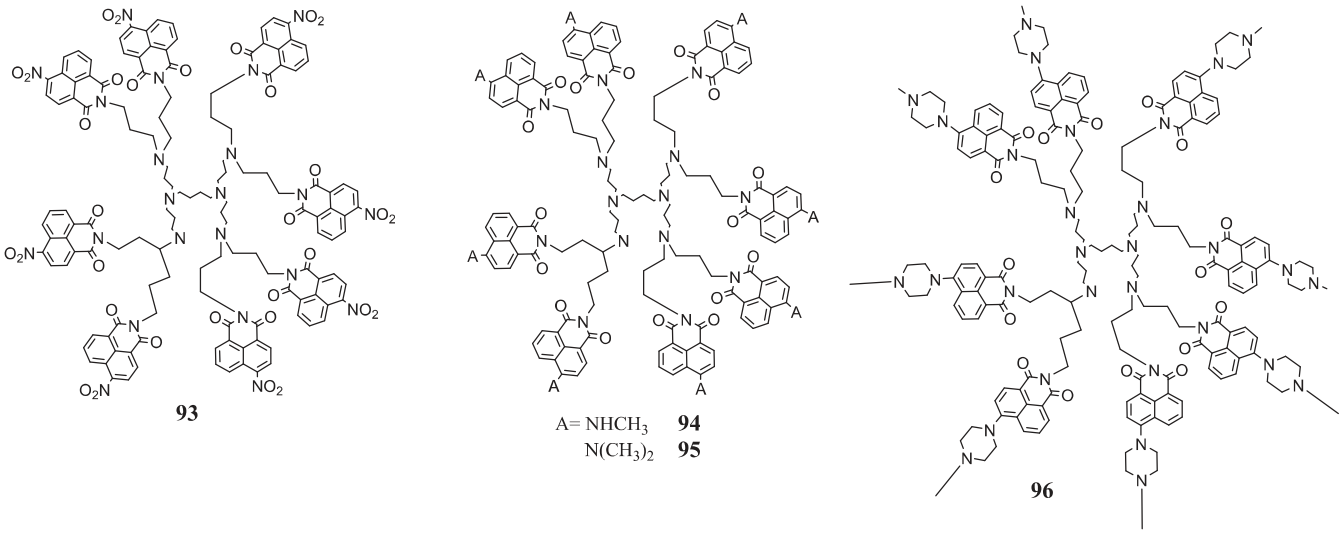

Fig. 25. 1,8-Naphthalimide dendrimers.

λ_{abs} of the **96** dendrimer was not strongly dependant on the solvent polarity. The value of ε in the long-wavelength band region of the absorption spectra of **96** dendrimer was greater than 10000 mol l^{-1} cm^{-1}, indicating the π,π* character of the $S_0 \rightarrow S_1$ transition. The value of ε for the dendrimer was ~8 fold larger than that of 4-*N*-methylpiperazine-*N*-allyl-1,8-naphthalimide [60], suggesting no ground state interaction between the naphthalimide moieties [61]. A hipsochromic shift was observed for the spectra of the solutions in non polar solvents compared to those of the solutions in the polar organic solvents ($\Delta\lambda_{abs}$= 20 nm). For the solid film of dendrimer **95** λ_{abs} was bathochromically shifted as compared to those of the solutions in organic solvents. This was probably due to the fixed dendrimer structure and to the limited possibility of conformational changes. The hypsochromic shift of the absorption and fluorescence maxima in the case of **95** compared with **94** can be explained by the steric interaction between one of the methyl groups of the 4-dimethylamino substituent at C-4 position and the hydrogen atom at C-5 position (the peri effect). Φ_F was considerably higher for the solutions in nonpolar media of all the dendrimers. Φ_F values were lower in the case of dendrimer **95**. Φ_F of **96** dendrimer was between 0.005 and 0.69.

Du and co-workers [62] synthesized a series dendrimers (**97**–**105**) containing naphthalimide mopieties (Fig. 26).

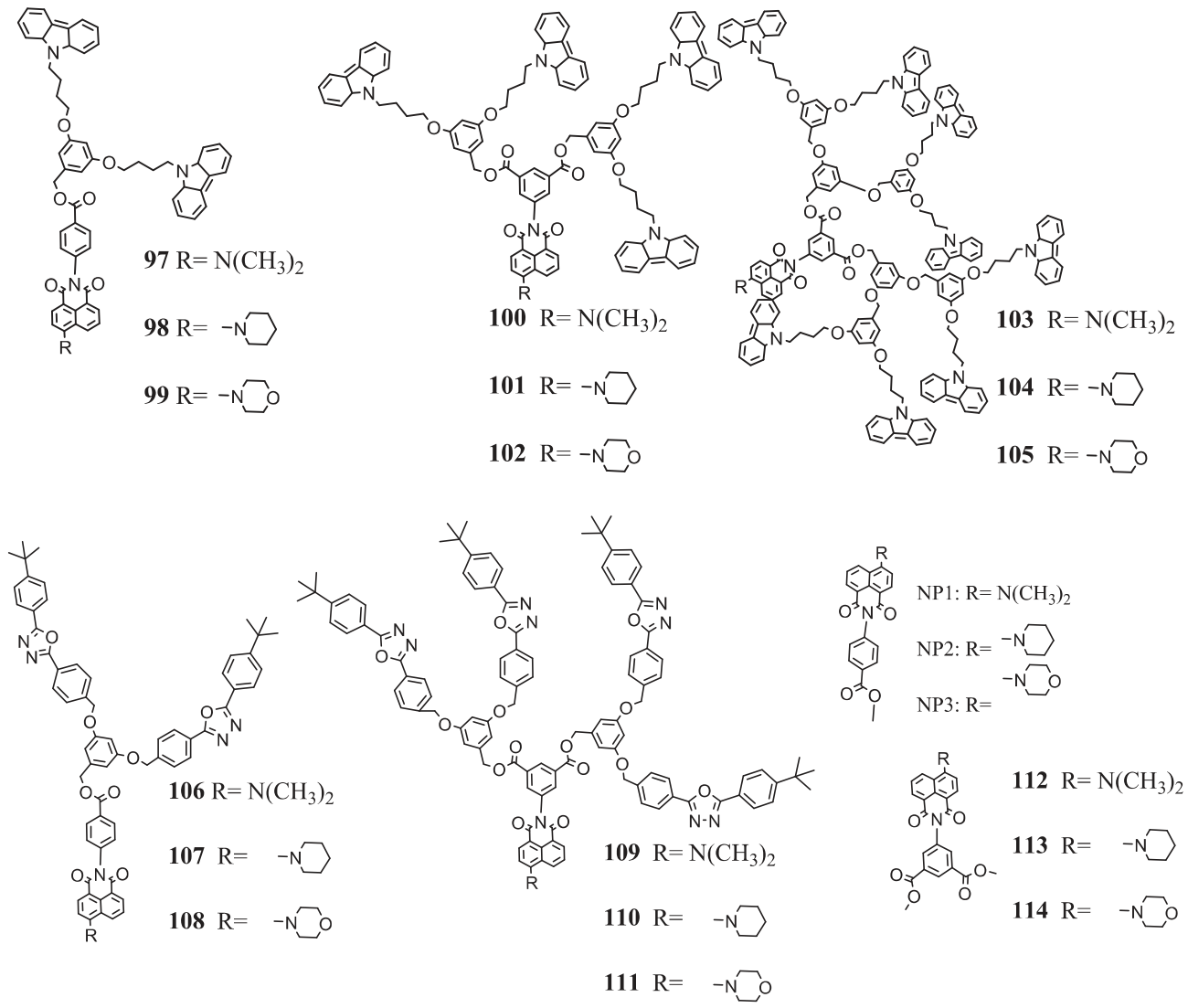

Fig. 26. 1,8-Naphthalimide dendrimers.

The absorption of **NP1-NP3** of the films shifted bathochromically compared with **NP1-NP3** in solution, due to the aggregation effect. Compared with their absorption in the solution, the absorption red shifts of **99**, **102**, and **105** were 25, 13, and 12 nm, respectively. The EA_{CV} and IP_{CV} energy values for all dendrimers were in the range of 5.18–5.67, and -2.97 – -3.04, respectively. T_g of **108** and **110** at 139 and 102 °C, respectively. A single-layer OLED was designed with the configuration of

(ITO/PEDOT(65 nm)/dendrimers/Ba (4 nm)/Al (150 nm)). EL results demonstrated that these dendrimers could be utilized as a promising active non-doping emitters with charge carrier-transporting ability.

3. Summary

The review shows that wide possibilities of changing the thermal, electrochemical, optical, photophysical, electroluminescent, and photoelectrical properties of 1,8-naphthalimide derivatives can be materialized by introducing different electron-donating or electron-accepting substituents at the C-4 position in the 1,8-naphthalimide moiety. 1,8-Naphthalimide-based compounds display a wide range of interesting fluorescence properties, including high fluorescence quantum yields in solutions and solid films, good optical properties, high thermal (up to 489 ^{o}C) and chemical stabilities. Many 4-substituted 1,8-naphthalimide derivatives were capable to form glasses (up to 254 ^{o}C) with good morphological stability. Moreover, some of them displayed relatively good charge-transporting capabilities that were appropriated for balanced carrier injection in organic light-emitting diodes. At the same time, derivatives 1,8-naphthalimide have found application in other optoelectronic devices, such as organic solar cells as well as in memory devices. The design and modification of the dendrimers with fluorescent 1,8-naphthalimide units could produce new interesting optical and photophysical properties.

Declaration of competing interest

The authors declared that they have no conflicts of interest to this work.

We declare that we do not have any commercial or associative interest that represents a conflict of interest in connection with the work submitted.

Acknowledgments

DG acknowledges to the ERDF PostDoc project No. 1.1.1.2/VIAA/1/16/177.

References

[1] P. Kucheryavy, G. Li, S. Vyas, C. Hadad, K.D. Glusac, Electronic properties of 4-substituted naphthalimides, J. Phys. Chem. A. 113 (2009) 6453–6461. doi:10.1021/jp901982r.

[2] S. Dhar, S. Singha Roy, D.K. Rana, S. Bhattacharya, S. Bhattacharya, S.C. Bhattacharya, Tunable solvatochromic response of newly synthesized antioxidative naphthalimide derivatives: Intramolecular charge transfer associated with hydrogen bonding effect, J. Phys. Chem. A. 115 (2011) 2216–2224. doi:10.1021/jp1117773.

[3] R.F. Jin, S.S. Tang, W.D. Sun, Rational design of donor-π-acceptor n-butyl-1,8-naphthalimide-cored branched molecules as charge transport and luminescent materials for organic light-emitting diodes, Tetrahedron. 70 (2014) 47–53. doi:10.1016/j.tet.2013.11.042.

[4] M.S. Alexiou, V. Tychopoulos, S. Ghorbanian, J.H.P. Tyman, R.G. Brown, P.I. Brittain, The UV-visible absorption and fluorescence of some substituted 1,8-naphthalimides and naphthalic anhydrides, J. Chem. Soc. Perkin Trans. 2. (1990) 837–842. doi:10.1039/p29900000837.

[5] D. Srikun, E.W. Miller, D.W. Domaille, C.J. Chang, An ICT-based approach to ratiometric fluorescence imaging of hydrogen peroxide produced in living cells, J. Am. Chem. Soc. 130 (2008) 4596–4597. doi:10.1021/ja711480f.

[6] F. Cacialli, R.H. Friend, C.M. Bouché, P. Le Barny, H. Facoetti, F. Soyer, P. Robin, Naphthalimide side-chain polymers for organic light-emitting diodes: Band-offset engineering and role of polymer thickness, J. Appl. Phys. 83 (1998) 2343–2356. doi:10.1063/1.366977.

[7] W. Zhu, M. Hu, Y. Wu, T. He, R.G. Sun, A.J. Epstein, Novel luminescent carbazole-naphthalimide dyads for single-layer electroluminescent device, Synth. Met. 119 (2001) 547–548. doi:10.1016/S0379-6779(00)01073-0.

[8] H. Tian, J. Su, K. Chen, T.C. Wong, Z.Q. Gao, C.S. Lee, S.T. Lee, Electroluminescent property and charge separation state of bis-naphthalimides, Opt. Mater. (Amst). 14 (2000) 91–94. doi:10.1016/S0925-3467(99)00112-3.

[9] L.G.F. Patrick, A. Whiting, Synthesis and application of some polycondensable flourescent dyes, Dyes Pigments. 52 (2002) 137–143. doi:10.1016/S0143-7208(01)00087-0.

[10] E. Martin, R. Weigand, A. Pardo, Solvent dependence of the inhibition of intramolecular charge-transfer in N-substituted 1,8-naphthalimide derivatives as dye lasers, J. Lumin. 68 (1996) 157–164. doi:10.1016/0022-2313(96)00008-7.

[11] Z.F. Tao, X. Qian, Naphthalimide hydroperoxides as photonucleases: Substituent effects and structural basis, Dyes Pigments. 43 (1999) 139–145. doi:10.1016/S0143-7208(99)00037-6.

[12] W.W. Stewart, Synthesis of 3,6-disulfonated 4-aminonaphthalimides, J. Am. Chem. Soc. 103 (1981) 7615–7620. doi:10.1021/ja00415a033.

[13] C.M. Bouché, P. Berdagué, H. Facoetti, P. Robin, P. Le Barny, M. Schott, Side-chain electroluminescent polymers, Synth. Met. 81 (1996) 191–195. doi:10.1016/S0379-6779(96)03767-8.

[14] W. Zhu, M. Hu, R. Yao, H. Tian, A novel family of twisted molecular luminescent materials containing carbazole unit for single-layer organic electroluminscent devices, J. Photochem. Photobiol. A Chem. 154 (2003) 169–177. doi:10.1016/S1010-6030(02)00325-8.

[15] H. Tian, J. Gan, K. Chen, J. He, L.S. Qun, Y.H. Xiao, Positive and negative fluorescent imaging induced by naphthalimide polymers, J. Mater. Chem. 12 (2002) 1262–1267. doi:10.1039/b200509c.

[16] T. Gunnlaugsson, C.P. McCoy, R.J. Morrow, C. Phelan, F. Stomeo, Towards the development of controllable and reversible `on-off` luminescence switching in soft-matter; synthesis and spectroscopic investigation of 1,8-naphthalimide-based PET (photoinduced, Arkivoc. 2003 (2003) 216–228.

[17] I.K. Grabtschev, I.T. Moneva, E. Wolarz, D. Bauman, New unsaturated 1,8-naphthalimide dyes for use in nematic liquid crystals, Zeitschrift Fur Naturforsch. - Sect. A J. Phys. Sci. 51 (1996) 1185–1191. doi:10.1515/zna-1996-1207.

[18] E.B. Veale, D.O. Frlmannsson, M. Lawler, T. Gunnlaugsson, 4-Amino-1,8-naphthalimide-based tröger's bases as high affinity DNA targeting fluorescent supramolecular scaffolds, Org. Lett. 11 (2009) 4040–4043. doi:10.1021/ol9013602.

[19] F. Cosnard, V. Wintgens, A new fluoroionophore derived from 4-amino-N-methyl-1,8-naphthalimide, Tetrahedron Lett. 39 (1998) 2751–2754. doi:10.1016/S0040-4039(98)00302-5.

[20] J.E. Rogers, L.A. Kelly, Nucleic acid oxidation mediated by naphthalene and benzophenone imide and diimide derivatives: Consequences for DNA redox chemistry, J. Am. Chem. Soc. 121 (1999) 3854–3861. doi:10.1021/ja9841299.

[21] A. Islam, C.C. Cheng, S.H. Chi, S.J. Lee, P.G. Hela, I.C. Chen, C.H. Cheng, Aminonaphthalic anhydrides as red-emitting materials: Electroluminescence, crystal structure, and photophysical properties, J. Phys. Chem. B. 109 (2005) 5509–5517. doi:10.1021/jp044669u.

[22] J.X. Yang, X.L. Wang, X.M. Wang, L.H. Xu, The synthesis and spectral properties of novel 4-phenylacetylene-1,8-naphthalimide derivatives, Dyes Pigments. 66 (2005) 83–87. doi:10.1016/j.dyepig.2004.07.015.

[23] J.X. Yang, X.L. Wang, A. Tusong, L.H. Xu, Studies on the synthesis and spectral properties of novel 4-benzofuranyl-1,8-naphthalimide derivatives, Dyes Pigments. 67 (2005) 27–33. doi:10.1016/j.dyepig.2004.09.017.

[24] J.L. Magalhães, R. V. Pereira, E.R. Triboni, P. Berci Filho, M.H. Gehlen, F.C. Nart, Solvent effect on the photophysical properties of 4-phenoxy-N-methyl-1,8-naphthalimide, J. Photochem. Photobiol. A Chem. 183 (2006) 165–170. doi:10.1016/j.jphotochem.2006.03.012.

[25] W. Jiang, Y. Sun, X. Wang, Q. Wang, W. Xu, Synthesis and photochemical properties of novel 4-diarylamine-1,8-naphthalimide derivatives, Dyes Pigments. 77 (2008) 125–128. doi:10.1016/j.dyepig.2007.03.017.

[26] S.O. Jung, W. Yuan, J.U. Ju, S. Zhang, Y.H. Kim, J.T. Je, S.K. Kwon, A new orange-light-emitting materials based on (N-naphthyl)-1,8-naphthalimide for OLED applications, Mol. Cryst. Liq. Cryst. 514 (2009) 45–54. doi:10.1080/15421400903217751.

[27] L. Wang, Y. Shi, Y. Zhao, H. Liu, X. Li, M. Bai, Push-pull 1,8-naphthalic anhydride with multiple triphenylamine groups as electron donor, J. Mol. Struct. 1056–1057 (2014) 339–346. doi:10.1016/j.molstruc.2013.10.004.

[28] R. Ferreira, C. Baleizão, J.M. Muñoz-Molina, M.N. Berberan-Santos, U. Pischel, Photophysical study of bis(naphthalimide)-amine conjugates: Toward molecular design of excimer emission switching, J. Phys. Chem. A. 115 (2011) 1092–1099. doi:10.1021/jp110470h.

[29] Y. Wang, X. Zhang, B. Han, J. Peng, S. Hou, Y. Huang, H. Sun, M. Xie, Z. Lu, The synthesis and photoluminescence characteristics of novel blue light-emitting naphthalimide derivatives, Dyes Pigments. 86 (2010) 190–196. doi:10.1016/j.dyepig.2010.01.003.

[30] M. Zheng, A.M. Sarker, E. Elif Gürel, P.M. Lahti, F.E. Karasz, Structure-property relationships in light-emitting polymers: Optical, electrochemical, and thermal studies, Macromolecules. 33 (2000) 7426–7430. doi:10.1021/ma000865x.

[31] D. Gudeika, J. V. Grazulevicius, D. Volyniuk, G. Juska, V. Jankauskas, G. Sini, Effect of Ethynyl Linkages on the Properties of the Derivatives of Triphenylamine and 1,8-Naphthalimide, J. Phys. Chem. C. 119 (2015) 28335–28346. doi:10.1021/acs.jpcc.5b10163.

[32] J. Xiao, Z. Deng, Synthesis and electroluminescent characterization of a symmetric starburst orange-red light material, J. Lumin. 132 (2012) 2863–2867. doi:10.1016/j.jlumin.2012.05.016..

[33] D. Gudeika, A. Michaleviciute, J. V. Grazulevicius, R. Lygaitis, S. Grigalevicius, V. Jankauskas, A. Miasojedovas, S. Jursenas, G. Sini, Structure properties relationship of donor-acceptor derivatives of triphenylamine and 1,8-naphthalimide, J. Phys. Chem. C. 116 (2012) 14811–14819. doi:10.1021/jp303172b.

[34] W. Ren, H. Zhuang, Q. Bao, S. Miao, H. Li, J. Lu, L. Wang, Enhancing the coplanarity of the donor moiety in a donor-acceptor molecule to improve the efficiency of switching phenomenon for flash memory devices, Dyes Pigments. 100 (2014) 127–134. doi:10.1016/j.dyepig.2013.09.002.

[35] D. Gudeika, G. Sini, V. Jankauskas, G. Sych, J. V. Grazulevicius, Synthesis and properties of the derivatives of triphenylamine and 1,8-naphthalimide with the olefinic linkages between chromophores, RSC Adv. 6 (2016) 2191–2201. doi:10.1039/c5ra24820e.

[36] J.A. Mikroyannidis, S. Ye, Y. Liu, Electroluminesent divinylene- and trivinylene-molecules with terminal naphthalimide or phthalimide segments, Synth. Met. 159 (2009) 492–500. doi:10.1016/j.synthmet.2008.11.009.

[37] L.F. Santos, R.C. Faria, L. Gaffo, L.M. Carvalho, R.M. Faria, D. Gonçalves, Optical, electrochemical and electrogravimetric behavior of poly(1-methoxy-4-(2-ethyl-hexyloxy)-p-phenylene vinylene) (MEH-PPV) films, Electrochim. Acta. 52 (2007) 4299–4304. doi:10.1016/j.electacta.2006.12.014.

[38] Y. Wang, J. Zhou, X. Wang, X. Zheng, Z. Lu, W. Zhang, Y. Chen, Y. Huang, X. Pu, J. Yu, An efficient guest/host fluorescent energy transfer pair based on the naphthalimide skeleton, and its

application in heavily-doped red organic light-emitting diodes, Dyes Pigments. 100 (2014) 87–96. doi:10.1016/j.dyepig.2013.08.021.

[39] J.A. Gan, Q.L. Song, X.Y. Hou, K. Chen, H. Tian, 1,8-Naphthalimides for non-doping OLEDs: The tunable emission color from blue, green to red, J. Photochem. Photobiol. A Chem. 162 (2004) 399–406. doi:10.1016/S1010-6030(03)00381-2.

[40] D. Gudeika, R. Lygaitis, V. Mimaite, J. V. Grazulevicius, V. Jankauskas, M. Lapkowski, P. Data, Hydrazones containing electron-accepting and electron-donating moieties, Dyes Pigments. 91 (2011) 13–19. doi:10.1016/j.dyepig.2011.02.002.

[41] Y. Liu, F. Niu, J. Lian, P. Zeng, H. Niu, Synthesis and properties of starburst amorphous molecules: 1,3,5-tris(1,8-naphthalimide-4-yl)benzenes, Synth. Met. 160 (2010) 2055–2060. doi:10.1016/j.synthmet.2010.07.020.

[42] J. Zhang, G. Li, C. Kang, H. Lu, X. Zhao, C. Li, W. Li, Z. Bo, Synthesis of star-shaped small molecules carrying peripheral 1,8-naphthalimide functional groups and their applications in organic solar cells, Dyes Pigments. 115 (2015) 181–189. doi:10.1016/j.dyepig.2015.01.002.

[43] D. Gudeika, J.V. Grazulevicius, D. Volyniuk, R. Butkute, G. Juska, A. Miasojedovas, A. Gruodis, S. Jursenas, Structure-properties relationship of the derivatives of carbazole and 1,8-naphthalimide: Effects of the substitution and the linking topology, Dyes Pigments. 114 (2015) 239–252. doi:10.1016/j.dyepig.2014.11.013.

[44] D. Gudeika, A. Ivanauskaite, R. Lygaitis, V. Kosach, D. Volyniuk, R. Butkute, A.P. Naumenko, V. Yashchuk, J. V. Grazulevicius, Charge-transporting blue emitters having donor and acceptor moieties, J. Photochem. Photobiol. A Chem. 315 (2016) 121–128. doi:10.1016/j.jphotochem.2015.10.002.

[45] D. Gudeika, R.R. Reghu, J. V. Grazulevicius, G. Buika, J. Simokaitiene, A. Miasojedovas, S. Jursenas, V. Jankauskas, Electron-transporting naphthalimide-substituted derivatives of fluorene, Dyes Pigments. 99 (2013) 895–902. doi:10.1016/j.dyepig.2013.07.016.

[46] D. Gudeika, J.V. Grazulevicius, G. Sini, A. Bucinskas, V. Jankauskas, A. Miasojedovas, S. Jursenas, New derivatives of triphenylamine and naphthalimide as ambipolar organic semiconductors: Experimental and theoretical approach, Dyes Pigments. 106 (2014) 58–70. doi:10.1016/j.dyepig.2014.02.023.

[47] J.F. Lee, S.L.C. Hsu, Efficient white polymer-light-emitting-diodes based on polyfluorene end-capped with yellowish-green fluorescent dye and blended with a red phosphorescent iridium complex, Polymer (Guildf). 50 (2009) 2558–2564. doi:10.1016/j.polymer.2009.03.051.

[48] G. Tu, Q. Zhou, Y. Cheng, L. Wang, D. Ma, X. Jing, F. Wang, White electroluminescence from polyfluorene chemically doped with 1,8-napthalimide moieties, Appl. Phys. Lett. 85 (2004) 2172–2174. doi:10.1063/1.1793356.

[49] Y. Te Chang, S.L. Hsu, M.H. Su, K.H. Wei, Soluble phenanthrenyl-imidazole-presenting regioregular poh (3-octylthiophene) copolymers having tunable bandgaps for solar cell applications, Adv. Funct. Mater. 17 (2007) 3326–3331. doi:10.1002/adfm.200700423.

[50] J.F. Lee, S.L.C. Hsu, Green polymer-light-emitting-diodes based on polyfluorenes containing N-aryl-1,8-naphthalimide and 1,8-naphthoilene-arylimidazole derivatives as color tuner, Polymer (Guildf). 50 (2009) 5668–5674. doi:10.1016/j.polymer.2009.10.010.

[51] C. Xia, R.C. Advincula, Decreased aggregation phenomena in polyfluorenes by introducing carbazole copolymer units, Macromolecules. 34 (2001) 5854–5859. doi:10.1021/ma002036h.

[52] G. Tu, C. Mei, Q. Zhou, Y. Cheng, Y. Geng, L. Wang, D. Ma, X. Jing, F. Wang, Highly efficient pure-white-light-emitting diodes from a single polymer: Polyfluorene with naphthalimide moieties, Adv. Funct. Mater. 16 (2006) 101–106. doi:10.1002/adfm.200500028.

[53] J. Liu, J. Cao, S. Shao, Z. Xie, Y. Cheng, Y. Geng, L. Wang, X. Jing, F. Wang, Blue electroluminescent polymers with dopant-host systems and molecular dispersion features: Polyfluorene

as the deep blue host and 1,8-naphthalimide derivative units as the light blue dopants, J. Mater. Chem. 18 (2008) 1659–1666. doi:10.1039/b716234k.

[54] J. Liu, Q. Zhou, Y. Cheng, Y. Geng, L. Wang, D. Ma, X. Jing, F. Wang, The first single polymer with simultaneous blue, green, and red emission for white electroluminescence, Adv. Mater. 17 (2005) 2974–2978. doi:10.1002/adma.200501850.

[55] J. Liu, S. Shao, L. Chen, Z. Xie, Y. Cheng, Y. Geng, L. Wang, X. Jing, F. Wang, White electroluminescence from a single polymer system: Improved performance by means of enhanced efficiency and red-shifted luminescence of the blue-light-emitting species, Adv. Mater. 19 (2007) 1859–1863. doi:10.1002/adma.200602942.

[56] J. Feng Lee, S.L.C. Hsu, P.I. Lee, H. Yi Chuang, M. Lun Yang, J. Sue Chen, W. Yang Chou, A new intramolecular donor-acceptor polyfluorene copolymer for bulk heterojunction solar cells, Sol. Energy Mater. Sol. Cells. 94 (2010) 1166–1172. doi:10.1016/j.solmat.2010.03.002.

[57] L. Huo, C. He, M. Han, E. Zhou, Y. Li, Alternating copolymers of electron-rich arylamine and electron-deficient 2,1,3-benzothiadiazole: Synthesis, characterization and photovoltaic properties, J. Polym. Sci. Part A Polym. Chem. 45 (2007) 3861–3871. doi:10.1002/pola.22136.

[58] I. Grabchev, P. Mokreva, V. Gancheva, L. Terlemezyan, Synthesis and structural dependence of the functional properties of new green fluorescent poly(propyleneamine) dendrimers, J. Mol. Struct. 1038 (2013) 101–105. doi:10.1016/j.molstruc.2013.01.021.

[59] I. Grabchev, D. Staneva, S. Dumas, J.M. Chovelon, Metal ions and protons sensing properties of new fluorescent 4-N-methylpiperazine-1,8-naphthalimide terminated poly(propyleneamine) dendrimer, J. Mol. Struct. 999 (2011) 16–21. doi:10.1016/j.molstruc.2011.03.020.

[60] I. Grabchev, S. Sali, R. Betcheva, V. Gregoriou, New green fluorescent polymer sensors for metal cations and protons, Eur. Polym. J. 43 (2007) 4297–4305. doi:10.1016/j.eurpolymj.2007.07.036.

[61] T.C. Barros, P.B. Filho, V.G. Toscano, M.J. Politi, Intramolecular excimer formation from 1,8-N-alkyldinaphthalimides, J. Photochem. Photobiol. A Chem. 89 (1995) 141–146. doi:10.1016/1010-6030(95)04040-M.

[62] P. Du, W.H. Zhu, Y.Q. Xie, F. Zhao, C.F. Ku, Y. Cao, C.P. Chang, H. Tian, Dendron-functionalized macromolecules: Enhancing core luminescence and tuning carrier injection, Macromolecules. 37 (2004) 4387–4398. doi:10.1021/ma049754e.

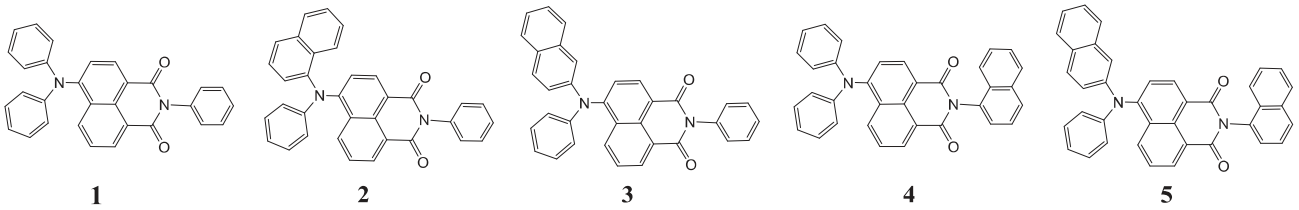

Fig. 1. Aryl- and 4-aryloxy-substituted naphthalimides.

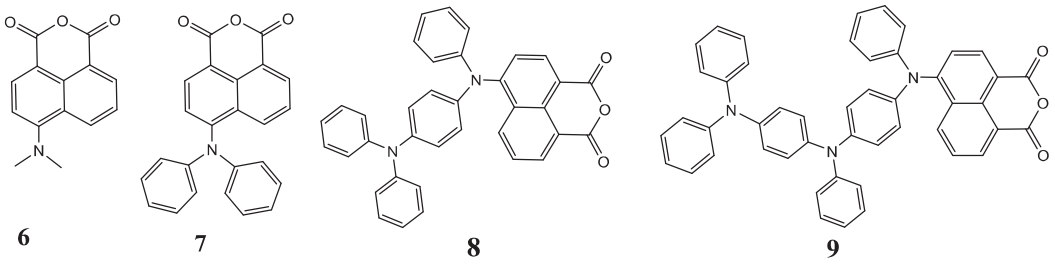

Fig. 2. Aryl- and 4-aryloxy-substituted naphthalimides.

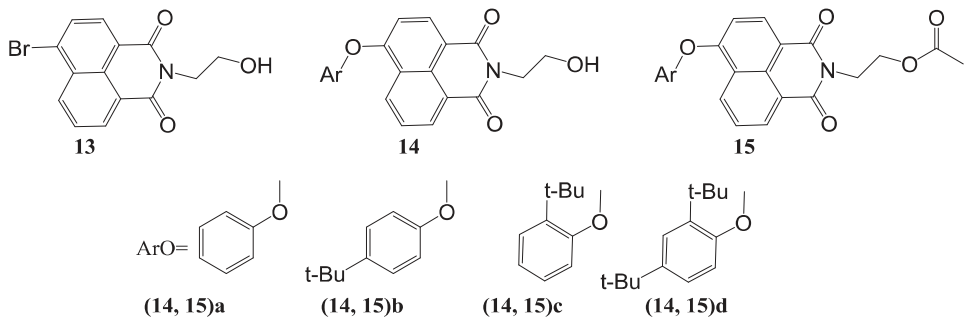

Fig. 3. Aryl- and 4-aryloxy-substituted naphthalimides.

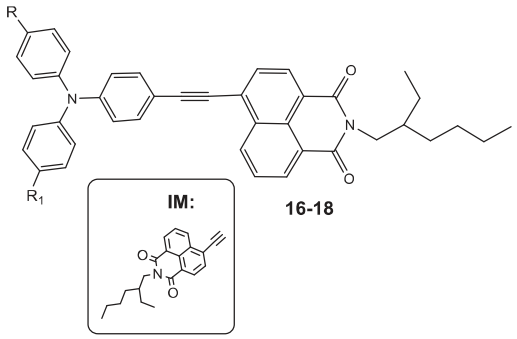

Comp.	R	R_1
16	H	H
17	H	IM
18	IM	IM

Fig. 4. 4-Ethynyl- and 4-ethenyl-substituted naphthalimides.

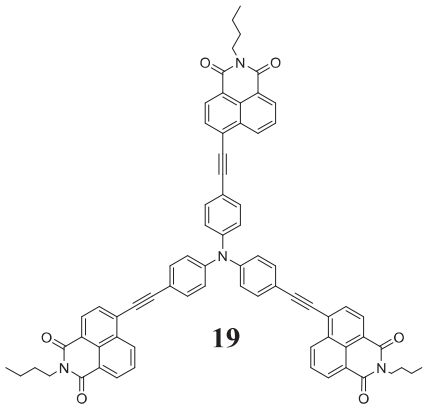

Fig. 5. 4-Ethynyl-substituted naphthalimide.

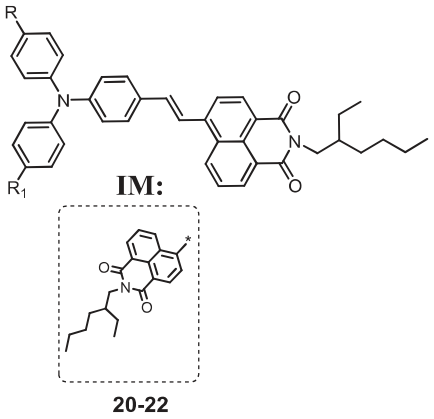

Comp.	**R**	**R_1**
20	H	H
21	H	CH=CH-**IM**
22	CH=CH-**IM**	CH=CH-**IM**

Fig. 6. 4-Ethynyl- and 4-ethenyl-substituted naphthalimides.

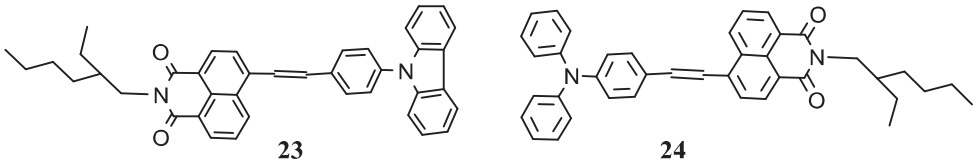

Fig. 7. 4-Ethynyl- and 4-ethenyl-substituted naphthalimides.

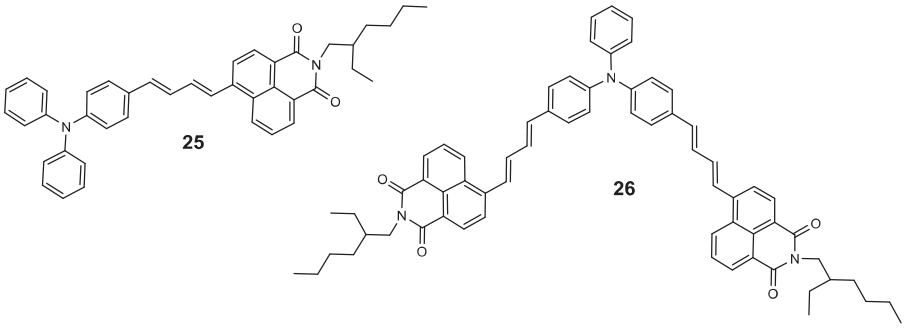

Fig. 8. 4-Ethynyl- and 4-ethenyl-substituted naphthalimides.

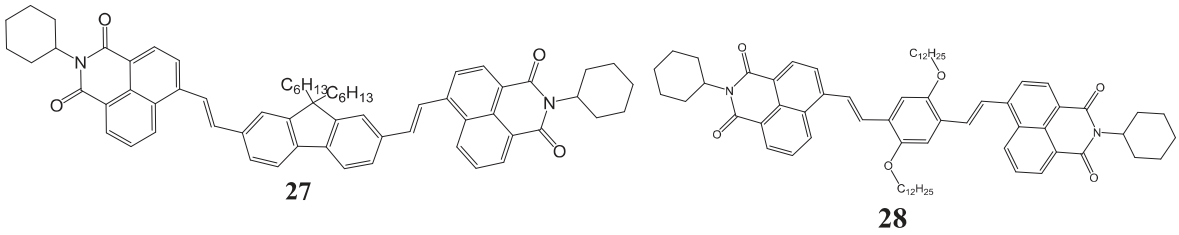

Fig. 9. 4-Ethynyl- and 4-ethenyl-substituted naphthalimides.

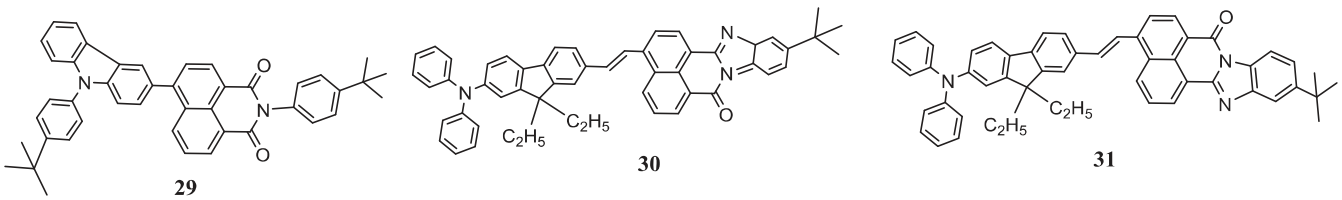

Fig. 10. 4-Ethynyl- and 4-ethenyl-substituted naphthalimides.

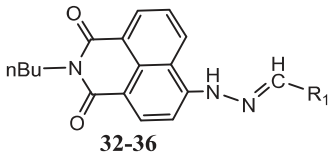

32-36

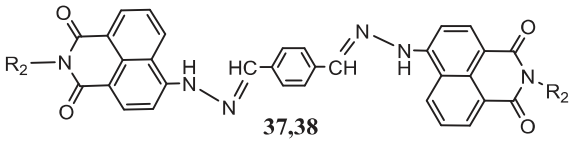

37,38

Comp.	**32**	**33**	**34**	**35**	**36**	**37**	**38**
R_1	-CH_3	-phenyl	4-methoxyphenyl	-anthracenyl	4-dimethylaminophenyl	–	–
R_2	–	–	–	–	–	*n*-butyl	*n*-$C_{12}H_{25}$

Fig. 11. Naphthalimide moiety containing hydrazones.

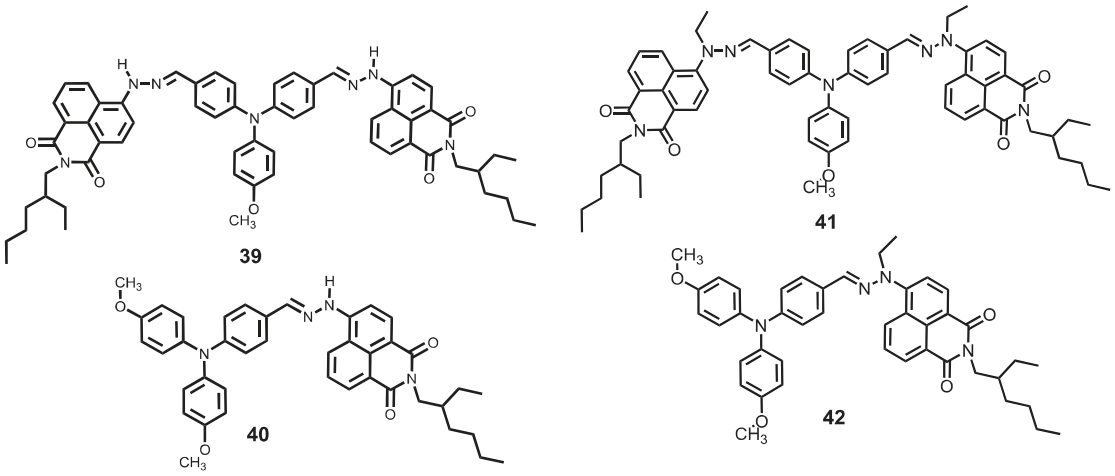

Fig. 12. Naphthalimide moiety containing hydrazones.

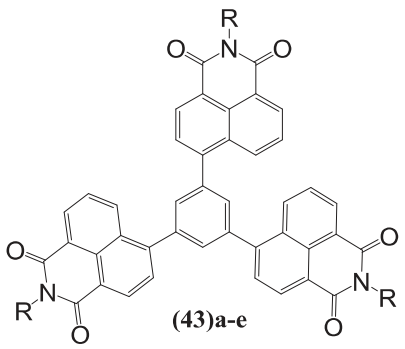

(43)a-e

43a, R= *n*-butyl
43b, R= *n*-hexyl
43c, R= 2-ethylhexyl
43d, R= 3,5-dimethylphenyl
43e, R= 9,9-dibuylfluorophenyl-2-yl

Fig. 13. 4-(Heter)oaromatic-substituted naphthalimides.

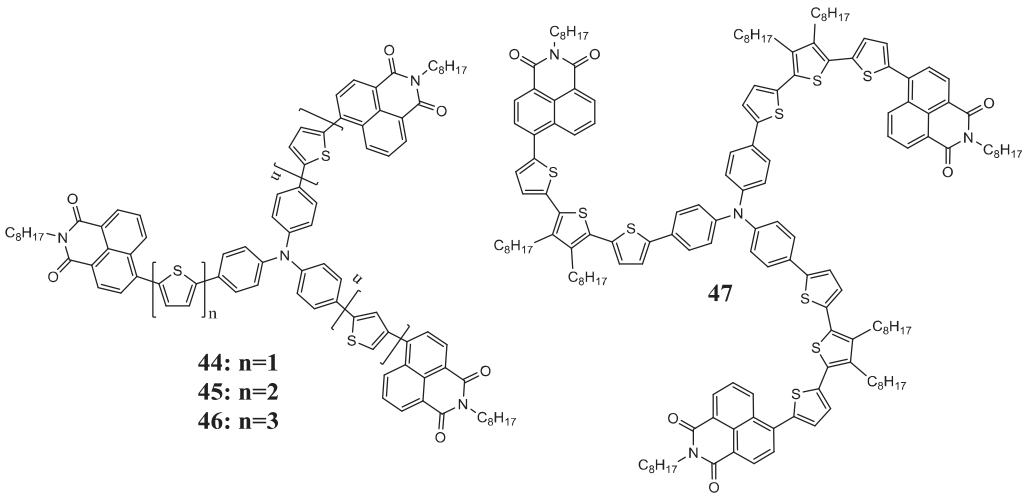

Fig. 14. 4-(Heter)oaromatic-substituted naphthalimides.

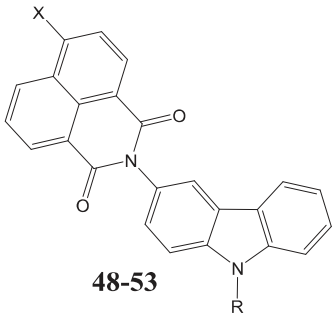

48-53

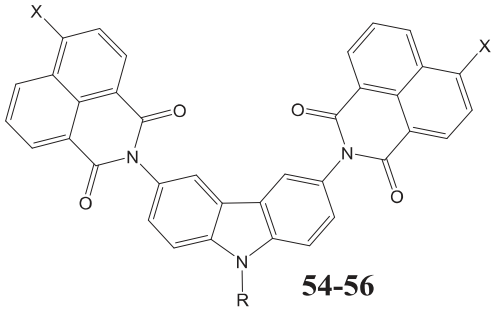

54-56

48, X=piperidino, R= C_2H_5
49, X= piperidino, R= C_6H_{13}
50, X=piperidino, R= $CH_2C_6H_5$
51, X=$N(CH_3)_2$, R= C_2H_5
52, X= $N(CH_3)_2$, R= C_6H_{13}
53, X= $N(CH_3)_2$, R= $CH_2C_6H_5$

54, X= piperidino, R= C_2H_5
55, X= piperidino, R= $CH_2C_6H_5$
56, X= $N(CH_3)_2$, R= C_2H_5

Fig. 15. 4-(Heter)oaromatic-substituted naphthalimides.

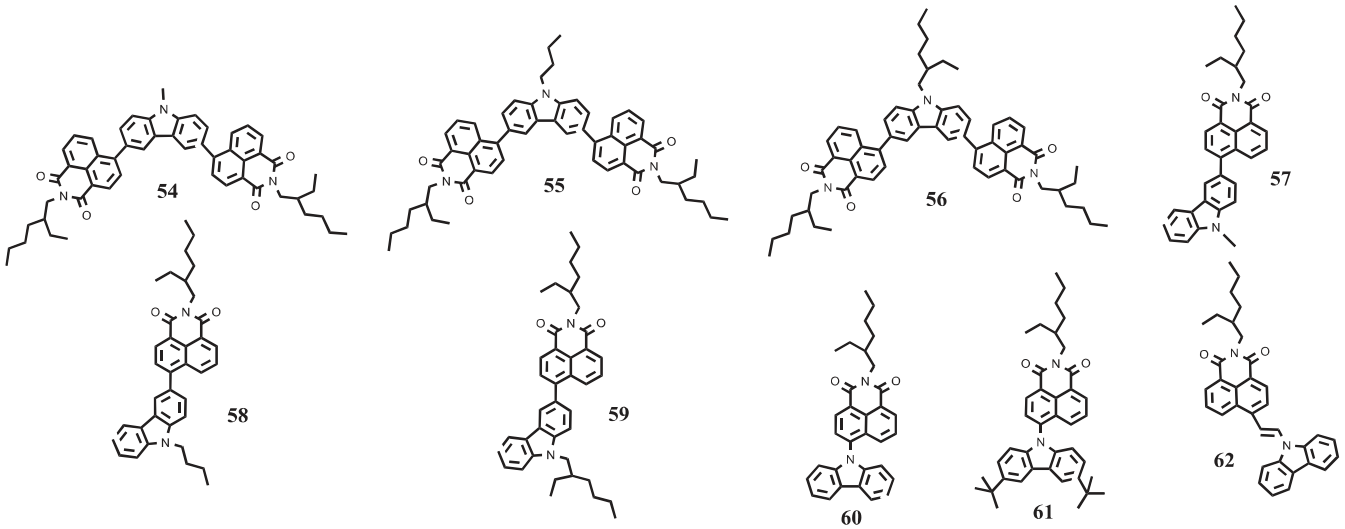

Fig. 16. 4-(Heter)oaromatic-substituted naphthalimides.

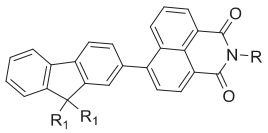

63-65

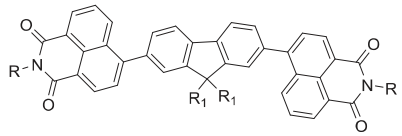

66-68

	R	R_1
63, 66	C_2H_5	$C_4H_9(C_2H_5)CHCH_2$
64, 67	$C_4H_9(C_2H_5)CHCH_2$	$C_4H_9(C_2H_5)CHCH_2$
65, 68	C_8H_{17}	C_8H_{17}

Fig. 17. 4-(Heter)oaromatic-substituted naphthalimides.

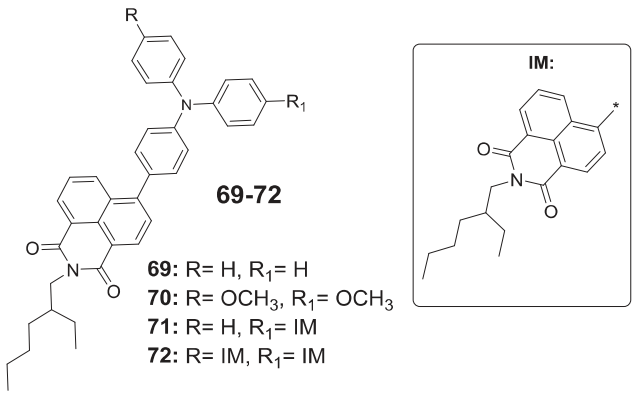

Fig. 18. 4-(Heter)oaromatic-substituted naphthalimides.

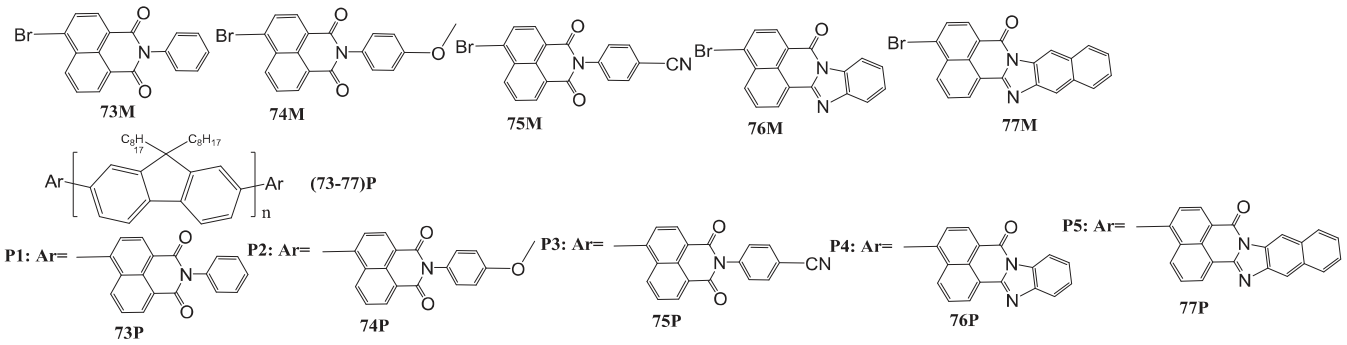

Fig. 19. 1,8-Naphthalimide polymers.

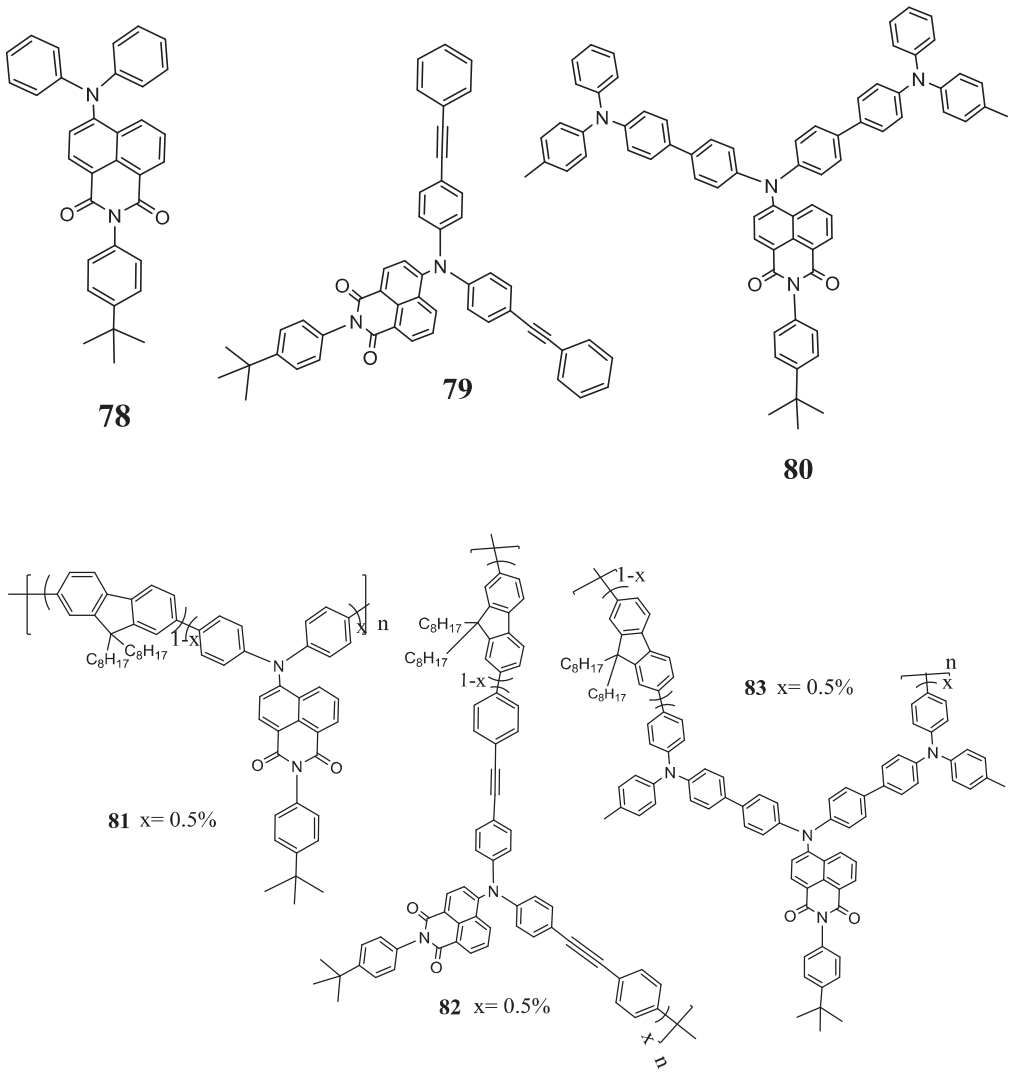

Fig. 20. 1,8-Naphthalimide polymers.

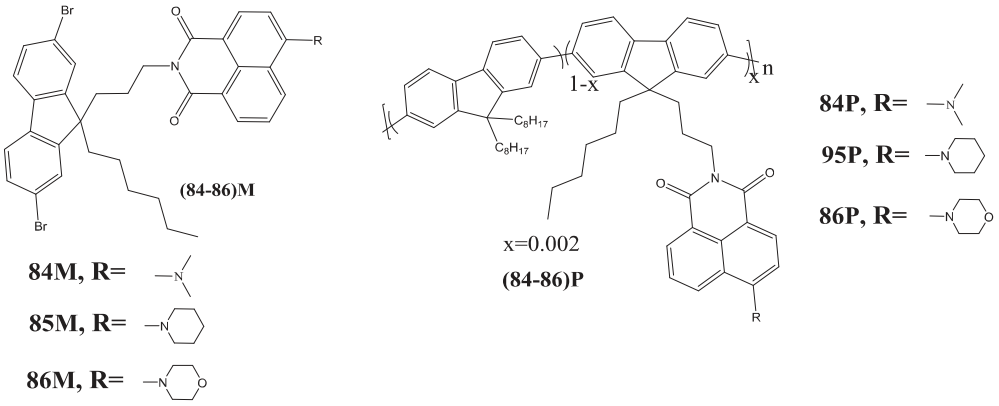

Fig. 21. 1,8-Naphthalimide polymers.

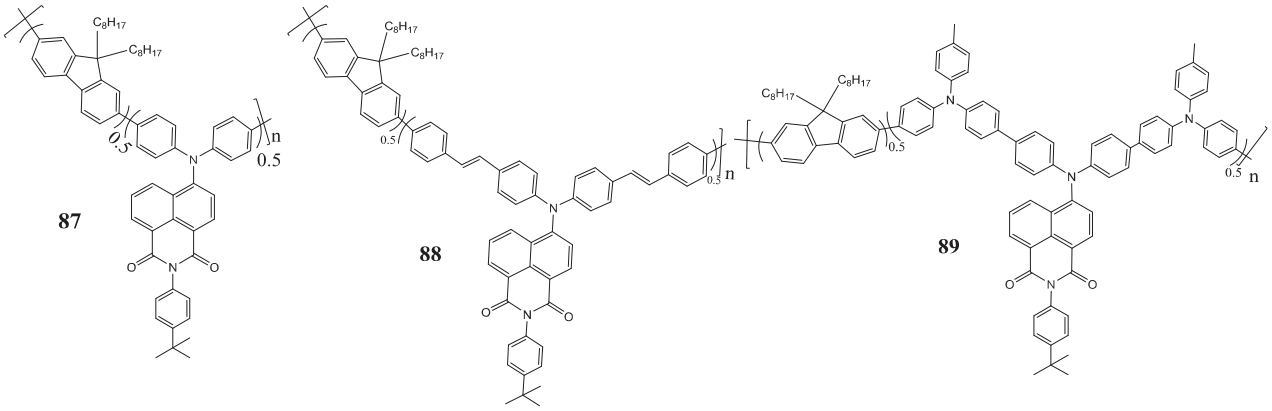

Fig. 22. 1,8-Naphthalimide polymers.

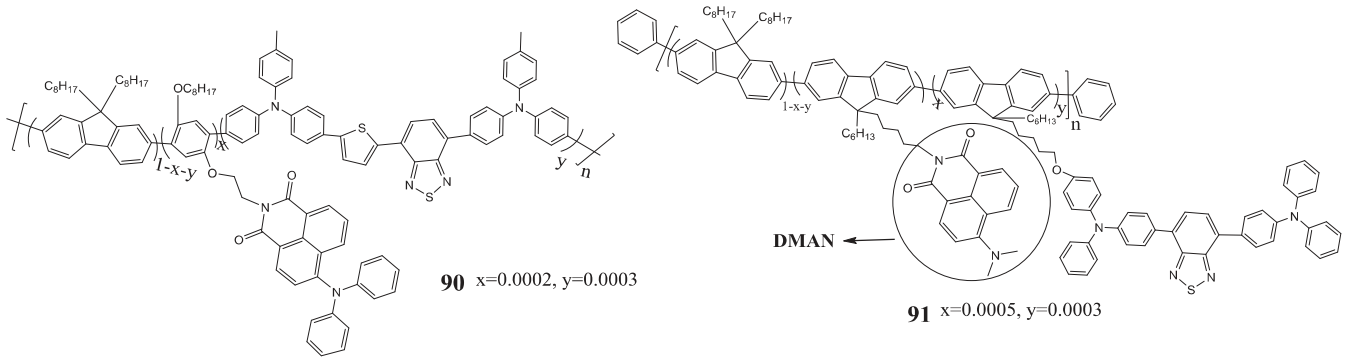

Fig. 23. 1,8-Naphthalimide polymers.

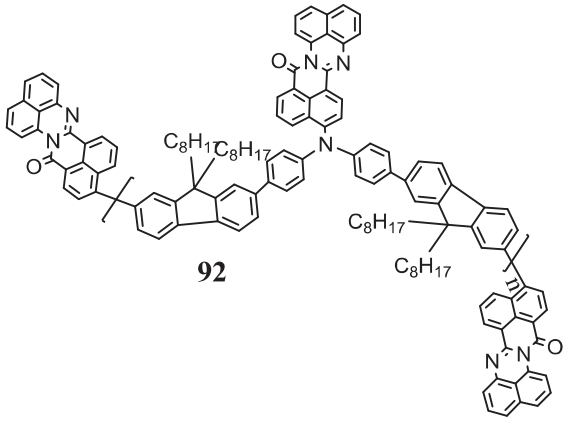

92

Fig. 24. 1,8-Naphthalimide polymer.

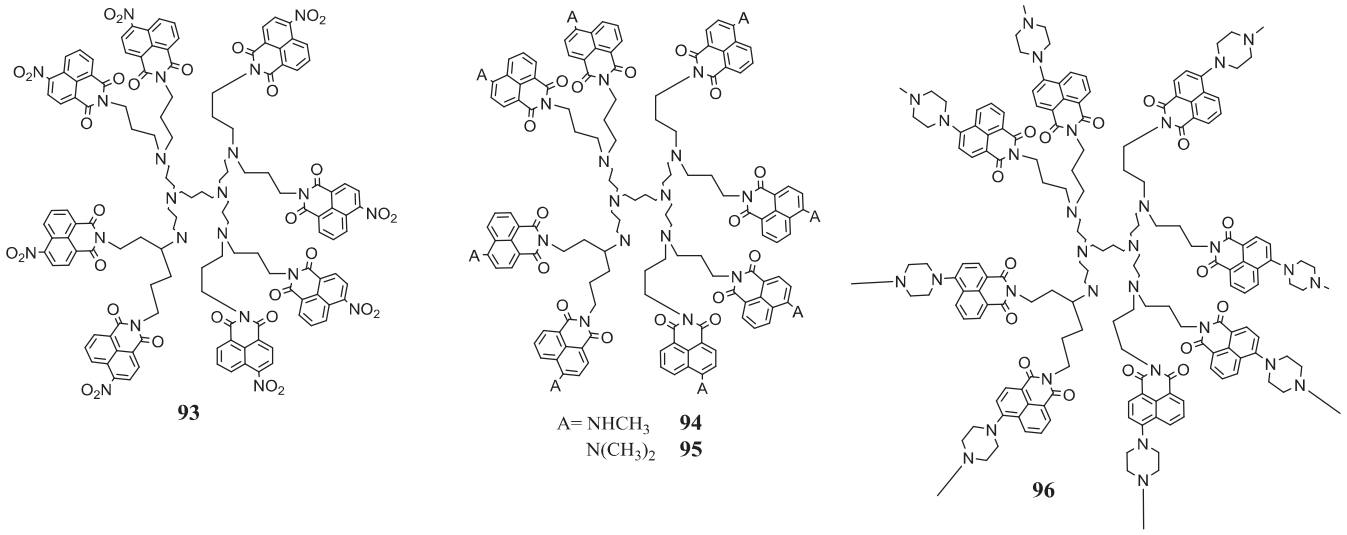

Fig. 25. 1,8-Naphthalimide dendrimers.

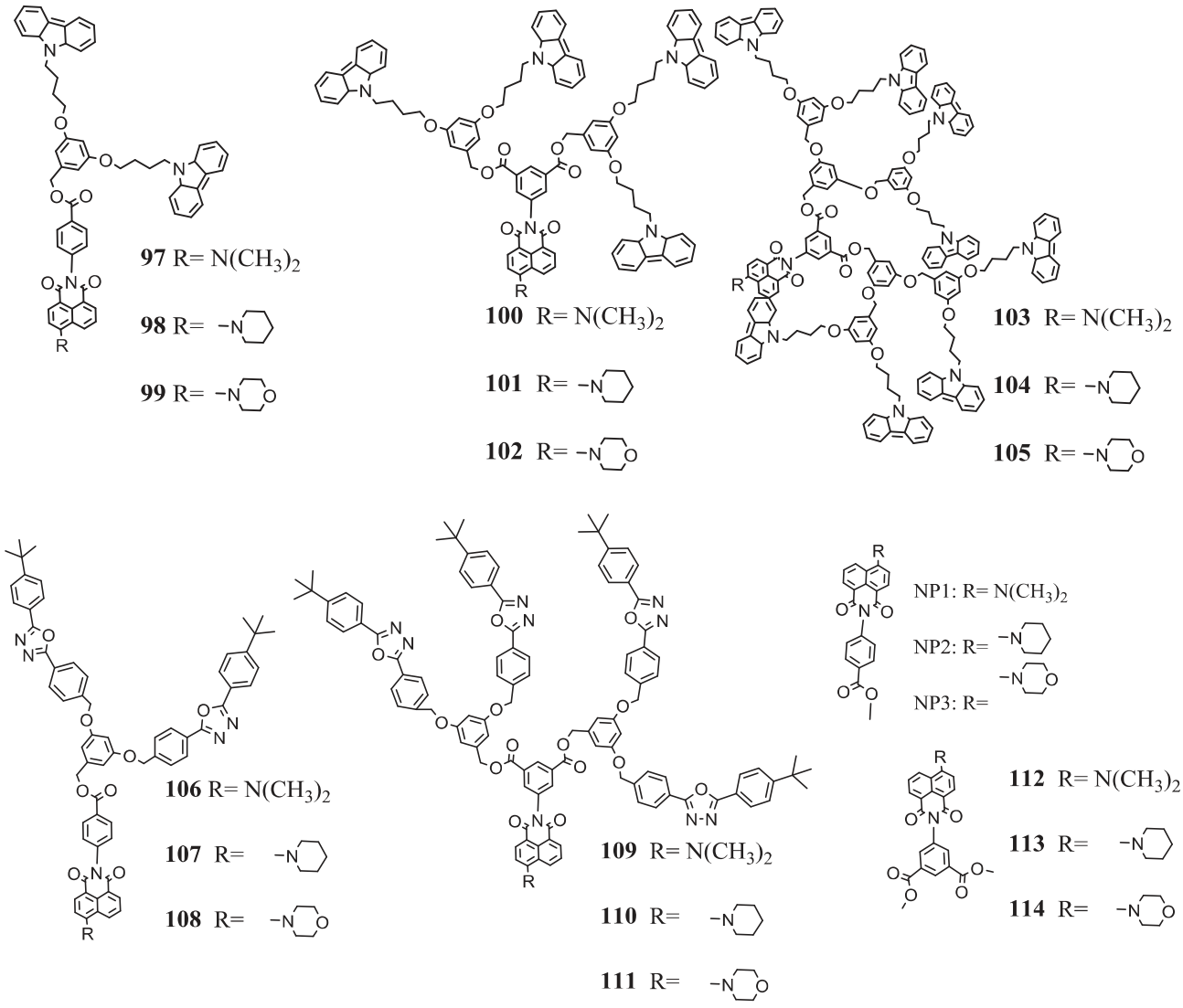

Fig. 26. 1,8-Naphthalimide dendrimers.

Table 1. Thermal, optical, photoelectrical and electrochemical characteristics of 1,8-naphthalimide derivatives.

Compound	T_g [°C]	T_m [°C]	T_{ID} [°C]	λ_{em}/ nm (Φ_F)	IP_{CV}, (eV)	EA_{CV}, (eV)	Mobility (μ_h), $cm^2/V s$
16	73	181	421	554 (0.17)	5.56	-3.18	10^{-3}
17	89	207	454	576 (0.25)	5.48	-3.16	10^{-2}
18	96	216	462	549 (0.011)	5.61	-3.29	-

T_g – glass-transition temperature; T_m – melting transition temperature; T_{ID} – temperature of the thermal decomposition; λ_{em} – maximum emission wavelength in solid films; Φ_F – fluorescence quantum yield in solid films; IP_{CV} – ionization potential; EA_{CV} – electron affinity; μ_h - hole mobility value at high electric fields.

Table 2. Thermal, optical, photoelectrical and electrochemical characteristics of 1,8-naphthalimide derivatives.

Molecule	T_g [°C][a] (2^{nd} heating)	T_{ID} [°C]	Film [nm]	λ_{em}	Φ_F film	I_p [eV]	Mobility (μ_h), $cm^2/V\ s$
20	55	431	624		0.18	5.75	10^{-3}
21	90	445	643		0.14	5.78	10^{-3}
22	107	448	652		0.09	5.80	10^{-4}

T_g – glass-transition temperature; T_{ID} – temperature of the onset of the thermal decomposition; λ_{em} – maximum emission wavelength in solid films; Φ_F – fluorescence quantum yield in solid films; I_p – ionization potential; μ_h - hole mobility value at high electric fields.

Table 3. Thermal, optical, photoelectrical and electrochemical characteristics of 1,8-naphthalimide derivatives.

Compound	T_g [°C]	T_{ID} [°C]	λ_{em} / nm (Φ_F)	IP_{CV} (eV)[(b)]	EA_{CV} (eV)[(b)]	μ_h (cm^2/Vs)
25	54	350	640 (0.034)	5.25	-3.20	2×10^{-3}
26	75	363	644 (0.028)	5.22	-3.18	2.16×10^{-4}

T_g – glass-transition temperature; T_{ID} – temperature of the onset of the thermal decomposition; λ_{em} – maximum emission wavelength in solid films; Φ_F – fluorescence quantum yield in solid films; IP_{CV} – ionization potential; EA_{CV} – electron affinity; μ_h - hole mobility value at high electric fields.

Table 4. Thermal, optical, photoelectrical and electrochemical characteristics of 1,8-naphthalimide derivatives.

Material	$T_{ID,}$ (°C)	$T_{g,}$ (°C)	$IP_{CV,}$ (eV)	$EA_{CV,}$ (eV)	E_g^{opt}, (eV)	E_g^{elc}, (eV)
39	275	142	5.06	-2.91	2.27	2.15
40	348	87	5.01	-2.91	2.27	2.10
41	268	73	5.06	-3	2.24	2.06
42	303	46	5.01	-3	2.25	2.01

T_g – glass-transition temperature; T_{ID} – decomposition temperature, IP_{CV} – ionization potential; EA_{CV} – electron affinity; E_g^{elc} – electrochemical band gap; E_g^{opt} – optical band gap.

Table 5. Thermal, optical, photoelectrical and electrochemical characteristics of carbazole derivative containing napthalimide moiety.

Material	T_g, (°C)	T_{ID}, (°C)	λ_{em}, (nm)	Φ_F	IP_{CV}, (eV)	EA_{CV}, (eV)	Mobility (μ_h), $cm^2/V\ s$
54	101	476	541	<0.01	5.68	-2.94	1.43×10^{-6}
55	96	457	522	0.17	5.67	-2.95	2.37×10^{-6}
56	30	383	513	0.06	5.75	-2.94	0.87×10^{-6}
57	47	434	522	0.01	5.56	-2.94	1.6×10^{-6}
58	15	385	533	0.07	5.55	-2.93	-
59	-5	351	519	0.06	5.58	-2.92	-
60	40	373	501	0.10	5.76	-3.04	3×10^{-6}
61	48	417	537	<0.01	5.46	-3.01	0.47×10^{-6}
62	-	422	563	0.45	5.45	-3.00	0.14×10^{-6}

T_g – glass-transition temperature; T_{ID} – temperature of the thermal decomposition; λ_{em} – maximum emission wavelength in solid films; Φ_F – fluorescence quantum yield in solid films; IP_{CV} – ionization potential; EA_{CV} – electron affinity; μ_h - hole mobility value of the order of 10^{-6} cm^2/Vs at the electric fields in the range from $(3.6\text{-}8.1)\times10^5$ V/cm.

Table 6. Thermal, optical, photoelectrical and electrochemical characteristics of carbazole derivative containing napthalimide moiety.

Material	$T_{g,}$ (°C)	$T_{ID,}$ (°C)	$\lambda_{em,}$ (nm)	Φ_F	Mobility (μ_e), $cm^2/V\ s$
63	30	392	474	0.23	3.8×10^{-5} (6.4×10^{-5} V/cm^{-1})
64	50	304	495	0.17	10^{-5} (6.4×10^{-5} V/cm^{-1})
65	-19	290	477	0.25	-
66	76	457	489	0.14	-
67	49	422	469	0.07	4×10^{-4} (6.4×10^{-5} V/cm^{-1})
68	59	441	480	0.25	1.2×10^{-3} (6.4×10^{-5} V/cm^{-1})

T_g – glass-transition temperature; T_{ID} – temperature of the onset of the thermal decomposition; λ_{em} – maximum emission wavelength in solid films; Φ_F – fluorescence quantum yield in solid films; μ_e - electron mobility value.

Table 7. Thermal, optical, photoelectrical and electrochemical characteristics of carbazole derivative containing napthalimide moiety.

Material	T_g, (°C)	T_{ID}, (°C)	λ_{em}, (nm)	Φ_F	I_p, (eV)	Mobility (μ_h), $cm^2/V\ s$	Mobility (μ_e), $cm^2/V\ s$
69	47	437	557	0.11	5.79	$3.7 \cdot 10^{-7}$	2.3×10^{-4}
70	45	429	630	0.10	5.57	1.1×10^{-4}	7.5×10^{-4}
71	76	448	569	0.16	5.93	4×10^{-7}	4.7×10^{-5}
72	93	483	570	0.23	6.01	2×10^{-8}[a]	-

T_g – glass-transition temperature; T_{ID} – temperature of the onset of the thermal decomposition; λ_{em} – maximum emission wavelength in solid films; Φ_F – fluorescence quantum yield in solid films; I_p - ionization potential was established from electron photoemission in air spectra; Hole and electron drift mobility values at electric field 1×10^6 V/cm. [a] Hole drift mobility value at electric field 3.6×10^5 V/cm.

Table 8. Properties of 1,8-naphthalimide derivatives.

Material	T_{ID}, (°C)	T_g, (°C)	IP_{CV}, (eV)	EA_{CV}, (eV)	Turn-on voltage, (V)	Brightness max, (cd/m^2)	Luminous efficiency max, (cd/A)
73	420	110	5.62	–2.14	22	930	0.19
74	424	112	5.67	–2.12	20	2890	0.28
75	421	110	5.68	–2.15	22	772	0.15
76	417	113	5.67	–2.24	6	11500	0.83
77	416	110	5.70	–2.36	7	6354	0.56

T_{ID} – temperature of the onset of the thermal decomposition; T_g – glass-transition temperature; IP_{CV} – ionization potential; EA_{CV} – electron affinity.

This paper is elaborated at the Centre of Excellence in Advanced Material Research and Technology Transfer of the Institute of Solid State Physics, University of Latvia executing project CAMART² that has received funding from the Horizon 2020 Framework Programme H2020-WIDESPREAD-01-2016-2017-TeamingPhase2 under grant agreement No. 739508